AD-A117 845 PITTSBURGH UNIV PA DEPT OF METALLURGICAL AND MATERI--ETC F/G 11/3
FUNDAMENTAL RESEARCH DIRECTED TO ADVANCED HIGH TEMPERATURE COAT--ETC(U)
APR 82 G H MEIER, F S PETTIT AFOSR-80-0089
UNCLASSIFIED AFOSR-TR-82-0548 NL

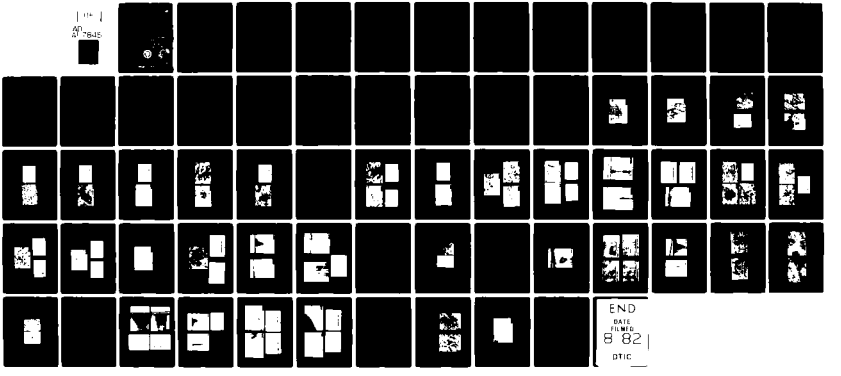

METALLURGICAL AND MATERIALS ENGINEERING

University of Pittsburgh
Pittsburgh, Pennsylvania 15261

APRIL 1, 1982

FUNDAMENTAL RESEARCH DIRECTED TO ADVANCED HIGH TEMPERATURE COATING SYSTEMS BEYOND THE CURRENT STATE-OF-THE-ART SYSTEMS

Second Annual Report
January 1-December 31, 1981

Prepared for

Air Force Office of Scientific Research
Contract No. AFOSR-80-0089

by

G. H. Meier

and

F. S. Pettit

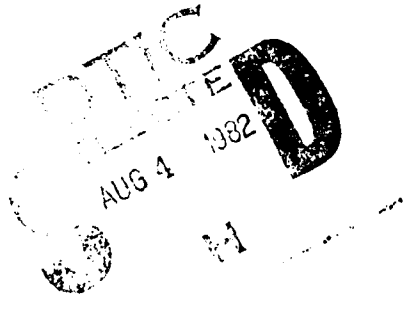

Metallurgical and Materials Engineering Department
Univeristy of Pittsburgh
Pittsburgh, PA 15261

Telephone Numbers (412) 624-5316
(412) 624-5300

Unclassified

SECURITY CLASSIFICATION OF THIS PAGE (When Data Entered)

REPORT DOCUMENTATION PAGE		READ INSTRUCTIONS BEFORE COMPLETING FORM
1. REPORT NUMBER AFOSR-TR- 82-0548	2. GOVT ACCESSION NO. AD-A117 845	3. RECIPIENT'S CATALOG NUMBER
4. TITLE (and Subtitle) "FUNDAMENTAL RESEARCH DIRECTED TO ADVANCED HIGH TEMPERATURE COATING SYSTEMS BEYOND THE CURRENT STATE-OF-THE-ART SYSTEMS"		5. TYPE OF REPORT & PERIOD COVERED Second Annual Report January 1-December 31, 1981 6. PERFORMING ORG. REPORT NUMBER
7. AUTHOR(s) G. H. MEIER and F. S. PETTIT		8. CONTRACT OR GRANT NUMBER(s) AFOSR-80-0089
9. PERFORMING ORGANIZATION NAME AND ADDRESS Metallurgical and Materials Engineering Department University of Pittsburgh Pittsburgh, PA 15261		10. PROGRAM ELEMENT, PROJECT, TASK AREA & WORK UNIT NUMBERS 61102F 2306/A2
11. CONTROLLING OFFICE NAME AND ADDRESS Department of the Air Force Office of Scientific Research (AFSC)/NE BOLLING AFB, DC 20332		12. REPORT DATE April 1, 1982 13. NUMBER OF PAGES 63
14. MONITORING AGENCY NAME & ADDRESS(if different from Controlling Office)		15. SECURITY CLASS. (of this report) Unclassified 15a. DECLASSIFICATION/DOWNGRADING SCHEDULE

16. DISTRIBUTION STATEMENT (of this Report)

Approved for public release;
distribution unlimited.

17. DISTRIBUTION STATEMENT (of the abstract entered in Block 20, if different from Report)

18. SUPPLEMENTARY NOTES

19. KEY WORDS (Continue on reverse side if necessary and identify by block number)

COATINGS, OXIDATION, NiCrALY ALLOYS, COATING ADHESION

20. ABSTRACT (Continue on reverse side if necessary and identify by block number)

The oxidation behavior of Ni-7.5 Si alloys has been studied in oxygen over the temperature range from 950 to 1150°C. The alloys exhibit significant transient oxidation but following this period oxidize at rates which are similar to those for Al_2O_3-forming systems. This slow rate is apparently due to the formation of a sealing layer of SiO_2 at the alloy/scale interface. The sealing layer appears to be slightly permeable to Ni which results in continued formation of NiO at the scale gase interface. Exposure of the alloys to gases with reduced oxygen pressure (P_{O_2} 10^{-5} atm) results in the formation of a

DD FORM 1 JAN 73 1473 EDITION OF 1 NOV 65 IS OBSOLETE

SECURITY CLASSIFICATION OF THIS PAGE (When Data Entered)

thin silica layer which appears to be impermeable to Ni. No detrimental effects of low P_{O_2} due to SiO evaporation were observed. These results suggest the possibility of imporving the oxidation behavior of Ni-Si alloys by controlled preoxidation at reduced oxygen pressures.

The effect of polishing of both plasma sprayed and PVD NiCoCrAlY coatings has been studied at 1100°C. It was found that exposing as-processed coatings resulted in the formation of adherent Al_2O_3 scales on both coatings. However, polishing away of the oxide film formed during processing resulted in coatings which on subsequent oxidation formed Al_2O_3 scales with poor adherence. The causes of this phenomenon need additional study.

The effects of ion implantation of Mg on the oxidation behavior of Ni-18 Cr-6 Al alloys has been investigated. It was found that the implantation resulted in a significant decrease in the amounts of transient oxide formed on both alloys. The implantation produced a measurable decrease in the overall rate of oxidation of Co-Cr-Al but not Ni-Cr-Al. The implantation did not produce an imporvement in scale adherence.

Techniques for quantitatively measuring the adherence of oxide scales are being developed and acoustic emission techniques are being developed to evaluate scale cracking during isothermal and cyclic oxidation. Preliminary results are described.

Finally the work planned for the third year of this program is outlined.

ABSTRACT

The oxidation behavior of Ni-7.5 Si alloys has been studied in oxygen over the temperature range from 950 to 1150°C. The alloys exhibit significant transient oxidation but following this period oxidize at rates which are similar to those for Al_2O_3-forming systems. This slow rate is apparently due to the formation of a sealing layer of SiO_2 at the alloy/scale interface. The sealing layer appears to be slightly permeable to Ni which results in continued formation of NiO at the scale gas interface. Exposure of the alloys to gases with reduced oxygen pressure ($P_{O_2} \approx 10^{-5}$ atm) results in the formation of a thin silica layer which appears to be impermeable to Ni. No detrimental effects of low P_{O_2} due to SiO evaporation were observed. These results suggest the possibility of improving the oxidation behavior of Ni-Si alloys by controlled preoxidation at reduced oxygen pressures.

The effect of polishing of both plasma sprayed and PVD NiCoCrAlY coatings has been studied at 1100°C. It was found that exposing as-processed coatings resulted in the formation of adherent Al_2O_3 scales on both coatings. However, polishing away of the oxide film formed during processing resulted in coatings which on subsequent oxidation formed Al_2O_3 scales with poor adherence. The causes of this phenomenon need additional study.

The effects of ion implantation of Mg on the oxidation behavior of Ni-18 Cr-6 Al alloys has been investigated. It was found that the implantation resulted in a significant decrease in the amounts of transient oxide formed on both alloys. The implantation produced a measurable decrease in the overall rate of oxidation of Co-Cr-Al but not Ni-Cr-Al. The implantation did not produce an improvement in scale adherence.

Techniques for quantitatively measuring the adherence of oxide scales are

being developed and acoustic emission techniques are being developed to evaluate scale cracking during isothermal and cyclic oxidation. Preliminary results are described.

Finally the work planned for the third year of this program is outlined.

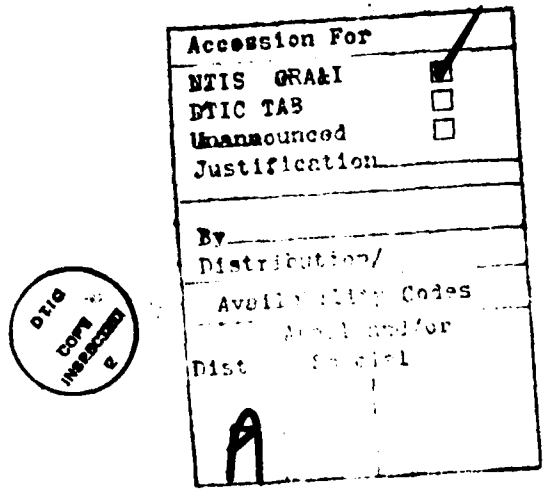

INTRODUCTION

The objective of this research is to define coatings compositions, structures and surface treatments that may be used to develop new advanced metallic coatings possessing improved high temperature oxidation resistance compared to the current state-of-the-art MCrAlY systems and diffusion aluminide coatings. The first Task of this program was directed towards determining the type of oxide scales which would be most effective for developing oxidation resistance in metallic coatings. This Task has been completed and it was concluded that only three systems had any potential for use as protection schemes against high temperature oxidation. These systems were MgO, SiO_2 and α-Al_2O_3. While MgO was considered to be a good barrier against oxidation, it was determined that it was exceedingly difficult to selectively oxidize this element in alloys due to its low solubility in most alloys. Magnesia therefore has not been considered any further as a means to obtain improved resistance to high temperature oxidation.

Task II involves attempts to optimize the protection for the best oxide systems, in particular, silica and α - Al_2O_3. Work on this Task has been performed during the second year of this program. The results obtained are presented and discussed in this report.

The third and final Task of this program is to consist of examining the effect of substrate composition on the oxidation degradation of selected coatings compositions where the compositions to be examined will be selected based upon the results obtained in Task II.

In this report the results obtained from studies concerned with the protectiveness of silica and α - Al_2O_3 scales will be presented by first considering the development and growth of silicon - containing oxide scales. The effects of surface preparation on α - Al_2O_3 development and adherence will then examined followed by

the results obtained by using ion implanted specimens. Finally, some of the techniques that have been worked upon in order to attempt to study oxide scale adhesion more effectively will be described.

RESULTS AND DISCUSSION

A. Alloys Forming Si-Containing Oxides

The work reported for the first year of this study[1] indicated that Si-rich oxides formed on Ni-7.5 Si* alloys had the potential to be as protective as α-Al_2O_3 scales. Therefore the study of Ni-Si alloys was continued during the second year. This study included evaluation of the oxidation kinetics over a range of temperatures, identification of reaction products, effects of reduced oxygen pressure, and the effect of increased Si concentration in the alloy.

In order to compare the rates of oxidation for alloys with silicon-containing scales to those for alloys upon which α-Al_2O_3 was formed, Ni-7.5 Si specimens were oxidized in 1 atm. oxygen at temperatures between 950 and 1150°C. The oxidation kinetics indicated that a substantial amount of transient oxidation occurred before the silicon-containing scale became continuous over the surfaces of the specimens. After about 20 hours of oxidation the weight change data for these specimens approximated a parabolic rate law. The parabolic rate constants that were obtained are compared to those for alloys with α-Al_2O_3 scales in Figure 1. The rate constants for the silicon-containing scales are larger than those for α-Al_2O_3 but the difference is not large. It is believed that lower rate constants for the silicon-containing scales may occur on alloys with smaller transient oxidation stages. Also, as will be discussed later, the alteration of the structure of the silicon containing oxide to minimize the outward migration of Ni may reduce the oxidation rates.

*All compositions are presented in weight percent.

The oxide scales formed on the Ni-7.5 Si specimens were examined using x-ray diffraction and scanning electron microscopy with energy dispersive x-ray analysis. The x-ray diffraction analysis did not yield conclusive results indicating only the presence of NiO. (However, x-ray diffraction of scales formed on Ni-10Si indicates a broad, low-angle peak which may indicate the presence of an amorphous SiO_2 layer).

Figure 2 shows the scale/gas interface for a Ni-7.5 Si specimen oxidized for 20 hours at 950°C. The surface consists of mounds of NiO and smoother areas indicated to contain both Ni and Si. Examination of the substrate structure, Figure 3, showed that the alloy had a cast structure consisting of Ni_3Si dendrites in a Ni-Si solid solution matrix. The distribution of oxide in Figure 2 appears to be related to the distribution of phases in the alloy suggesting that surface modification of the alloy may allow the amount of NiO formation to be reduced.

Figure 4 shows the morphology of the alloy-side of a spalled oxide flake. The corresponding EDAX spectrum indicates only the presence of Si suggesting that a SiO_2 - layer has covered at least part of the alloy surface.

Figure 5 shows the surface at the gas interface of a specimen exposed for 72 hours and indicates a larger amount of the surface is covered by the crystals which are indicated by x-ray diffraction and EDAX (Fig. 5d) to be NiO. Figure 6 shows the alloy side of a spalled oxide flake and EDAX (Fig. 6b) indicates a high Si-concentration. Figure 7 shows a portion of the alloy substrate from which the scale has spalled and indicates a low residual Si concentration. These results indicate that a protective SiO_2 scale covers the alloy fairly early during the oxidation but the depletion of Si from the underlying alloy results in migration of Ni through the scale to form NiO at the oxide gas interface.

The possibility of enhanced degradation of SiO_2-forming alloys at low oxygen pressures due to SiO evaporation was investigated by exposing alloys in tank argon

($P_{O_2} \approx 10^{-6} - 10^{5}$ atm). The weight changes for these specimens were extremely small indicating protective oxidation. Figure 8 shows the scale/gas interface of a specimen exposed for 48 hours at 1000°C. The surface is covered with a thin, adherent oxide containing a high concentration of Si. Therefore, there does not appear to be an adverse effect of reduced oxygen pressure and, in fact, the Si-rich oxide which forms is very adherent and appears to be a better barrier to Ni transport than scales formed at high oxygen pressures. This observation suggests possible improvement in the oxidation resistance of Ni-Si alloys by controlled preoxidation. The fact that the oxidation of the Ni-Si alloy was not adversely affected by the reduced oxygen pressure suggests that silicon alloys may not be as susceptible as pure silicon to accelerated oxidation resulting from gaseous SiO formation[3]. The reason for this condition is not known but the pressure of SiO over an alloy may be lower than that for pure silicon if the surface of the alloy becomes covered with pure nickel or a layer of NiO.

A Ni-10 Si alloy was prepared to evaluate the effect of increased Si concentration on the oxidation of Ni-Si alloys. The rate of oxidation of this alloy in air at 1000°C is presented in Figure 9. (The rates of Ni-7.5 Si, Ni-30 Cr and Ni-18 Cr - 6Al at 950°C are shown for comparison.) The weight change for the Ni-10 Si alloy is small but after 10 hours the rate of oxidation has become essentially linear and this linear rate has been shown to persist to the longest times studied (166 hrs.). X-ray diffraction of the oxide indicates NiO and a broad peak suggesting the presence of amorphous SiO_2. This alloy is still being studied but appears to be oxidizing by the continued formation of NiO at the scale/gas interface. It seems that a very slowly growing Si-rich layer has formed and that most of the weight gain is essentially due to a relatively slow "permeation" of Ni through this layer to form discontinuous NiO. A rough calculation using the measured linear rate and the data of Ghoshtagore[4] for the diffusion coefficient

of Ni in amorphorous SiO_2 indicates the SiO_2 layer must be less than 0.1 um thick if this mechanism is operative.

The results that have been obtained for the oxidation of alloys upon which silicon-containing scales are formed are not highly encouraging in regards to using of such scales as barriers to retard high temperature oxidation. Some silicon-containing scales have been observed to grow at rates comparable to the growth rates for α-Al_2O_3. Such scales, however, have been found to contain significant amounts of nickel and the nickel concentration in the scale appears to increase with time. In addition some of these silicon scales have been found to grow via linear rates. At the present time silicon-containing scales must be considered as a means for obtaining oxidation resistance in coatings but the results obtained to date indicate that such oxide barriers may not be effective barriers as α-Al_2O_3.

B. Oxidation of Plasma Spray and PVD NiCoCrAlY Coatings

Two NiCoCrAlY coatings of essentially the same composition were studied to evaluate the influence of coating technique on oxidation behavior. The coatings were plasma sprayed NiCoCrAlY (Ni - 22.8 Co - 17.9 Cr - 12.1 Al - 0.4 Y) and PVD NiCoCrAlY (Ni - 21.7 Co - 17.2 Cr - 12.1 Al - 0.4 Y). Both coatings were on IN - 100 erosion bars of approximately triangular cross sections. One side of each specimen cut from these bars was polished with 600 grit SiC, one side was left in the as-processed condition (thin oxide produced by 4 hr. H_2-anneal at 1080°C) and the third side formed the base which rested on an alumina boat. The specimens were oxidized in air at 1100°C for times of 1 and 24 hours. Figure 10 shows the scale gas interface of the unpolished side of the plasma-sprayed coating exposed for 1 hour. The scale is essentially Al_2O_3 but the presence of small amounts of Cr, Co, and Ni are also indicated. After 24 hours the scale is comprised only of Al_2O_3 (Figure 11). No scale spalling was observed for either specimen. The polished side of both specimens, however, exhibited considerable spalling on cooling (Figures 12 and 13) even though the scale compositions were essentially the same as

those on the unpolished sides. Observation of the 24 hour specimens in cross section (Figure 14) showed a dark oxide phase penetrating into the unpolished coating. EDAX analysis (Figure 15) indicated this phase was Al_2O_3. It is not yet clear if the formation of this phase is responsible for the better adherence on the unpolished sides of the specimens. Interestingly, no Y was detected in the scales on the plasma sprayed coatings.

The scale/gas interfaces of the unpolished PVD coatings exposed for 1 and 24 hours are shown in Figures 16 and 17. As in the case of the plasma spray coatings the 1 hour scale contains measurable amounts of Co, Ni, and Cr whereas the 24 hour scale is essentially Al_2O_3. However, both scales show the presence of Y. The distribution of Y in discrete nodules is shown clearly in Figure 18. No spalling was observed from the scales formed on the unpolished PVD coatings.

The scales on the polished sides of the 1 and 24 hour specimens are shown in Figures 19 and 20. Both specimens show extensive scale spalling and the presence of Y is much less evident in the scales. In fact, no Y was detected in the 1 hour scale. Evidently the polishing away of the oxide film formed during the hydrogen anneal renders the Y much less effective in providing scale adherence to the PVD coating. The cross-sections shown in Figures 21 and 22 also show that a much more uniform alumina grows on the unpolished surface.

The results of this section indicate that the initial exposure conditions can be critical in determining the long term oxidation behavior of both plasma sprayed and PVD coatings. Such results have been observed by those who work with coatings but the cause for these conditions has not been documented. In the present studies since polishing has been observed to produce some very significant effects on both α-Al_2O_3 development and adherence, systems and techniques appear to be available to describe the effects produced by coatings surface condition on α-Al_2O_3 scale development and adherence.

C. Effects of Ion-Implantation on High Temperature Oxidation

Previous work on this project[1] has shown that implantation of Mg ions into pure Ni produces a marked decrease in the subsequent oxidation rate. Therefore, the study has been continued to ascertain the effects of Mg-implantation on the oxidation behavior of Co-Cr-Al and Ni-Cr-Al alloys. Specimens of Co-18Cr-6Al and Ni-18 Cr-6Al were implanted with 150 kV Mg ions to a dose of 3.4×10^{16} ions/cm^2. Figure 23 shows the Mg concentration profile in pure Ni and, although not measured, the profiles in the Co- and Ni-alloys will be quite similar. The implantation also produces point defects by radiation damage. The concentration profile for these defects will have a similar shape to that for the Mg ions but has its maximum slightly nearer the specimen surface.

Figure 24 shows a transmission electron micrograph of the implanted region of a Co-18Cr-6Al alloy and the corresponding electron diffraction pattern. The alloy is seen to contain a high density of fine planar defects, probably twins, which give rise to streaking of the reflections in the diffraction pattern.

Figure 25 indicates that the implantation has resulted in a small, but distinct, decrease in the weight gain of Co-18Cr-6Al during oxidation at 950°C in pure oxygen. Metallographic analysis indicates that this decrease is due to the implantation virtually eliminating the transient oxidation period. Figure 26 shows a cross section of an unimplanted specimen and Figure 27 shows the corresponding EDAX spectra at the indicated locations. The external scale is seen to consist of Co- and Cr- rich oxides while the Al is oxidized internally. Figures 28 and 29 show a cross section through an implanted specimen and the corresponding EDAX spectra. Here the external scale is seen to contain a continuous layer of Al-oxide (Region 2) and the absence of internal oxidation is evident. The reduction in transient oxidation is the result of two factors: the presence of an oxygen active element (Mg) and the radiation damage which increases the alloy interdiffusion

coefficient. Both of these effects legislate in favor of the rapid formation of a continuous external layer of Al_2O_3. The relative importance of the two effects requires additional experiments involving implantation of ions such as Co whose only effect would be to produce radiation damage.

The implantation of Mg has little effect in scale spallation during cooling as seen in Figure 30. This morphology is virtually identical to that for unimplanted Co-18 Cr-6 Al reported previously.[1]

Figure 31 shows a transmission electron micrograph of the implanted region of a Ni-18 Cr-6 Al alloy. This microstructure is characterized by a high dislocation density and resembles that of a fairly heavily cold worked alloy. In this case, however, the implantation has a neglibile effect on the oxidation kinetics, as seen in Figure 32. Comparison of Figures 33 and 34 indicate that the implantation has eliminated the internal oxidation of Al in the alloy. This is likely the result of enhanced alloy interdiffusion due to the damage produced by implantation.

Comparison of Figures 35 and 36 indicates the implantation has altered the spalling pattern from Ni-18 Cr-6 Al. The scale spalls in small pieces from the unimplanted alloy[1] (Fig. 35) but spalls in large sheets from the Mg-implanted alloy. This is due to more uniform Al_2O_3 produced on the implanted alloy (Fig. 34.).

The results obtained with ion implantation show rather clearly that this technique affects α-Al_2O_3 scale development as well as adhesion. Such results have been obtained previously by other investigators. It is now necessary to describe how the ion implantation affects alloy oxidation behavior as it does and to determine how long lasting the ion implantation effects may be.

D. Studies of Scale Cracking and Adherence

A major factor in determining the life of high temperature alloys and coatings is the resistance of the oxide to cracking and spalling under both isothermal and cyclic conditions. The influence of oxygen active elements in improving oxide

adherence is now well documented. However, there are no techniques which allow a quantitative, or even semiquantitative, measurement of oxide adherence to be made. Such techniques would be useful both in elucidating oxidation mechanisms and in making comparisons of the relative adherence producted by different oxygen-active elements and surface treatments. Two techniques are being developed on the current project which are believed to offer potential for quantifying scale adherence and scale cracking. These techniques are (1) measuring the force required to pull an oxide from its metallic substrate and (2) using acoustic emission to monitor the extent of oxide cracking and scale/metal separation during both isothermal and cyclic exposures.

1. Measurement of Oxide/Metal Bond Strength

This test is essentially a tension test in which the load required to pull the oxide scale from the substrate surface is measured. The oxidized specimen is cemented between two steel blocks with a strong adhesive (Eastman 910 Adhesive). This assembly (Figure 37) is then loaded in tension in an Instron tensile machine.

It has been found that only scales with adhesive strengths less than 3000 psi can be pulled from their substrate since the failure occurs in the adhesive at higher loads. Also, perfect alignment of the blocks to avoid any shear stress components has been found essential to obtaining consistent results. One additional advantage of the technique is that both the underside of the scale and the alloy substrate can be examined by SEM or other techniques after the scale has been pulled from the substrate. Normally, if an oxide is adherent, the only way to study the underside of the scale is to dissolve away the substrate which precludes examination of the substrate.

Preliminary experiments have been performed on pure Ni, pure Co, Ni-22.5 Co - 15.5 Cr-14.5 Al-0.3 Y, and Ni-18 Cr-6 Al-1 Hf which have been oxidized in air. Short oxidation times and/or low oxidation temperatures produced thin oxide layers which were bound too tightly to the substrate to be pulled loose. In these cases failure occurred in the adhesive. Therefore, most of the specimens were oxidized for 70 to

200 hours at 1100 or 1150°C. The exception was Co which after oxidation for 72 hours at 975°C produced a scale which could be easily pulled from the substrate.

A pure Ni specimen oxidized for 82 hours at 1100°C required a stress of 700 psi to pull the oxide from the metal. This stress, however, is not a direct measure of the bond strength between metal and oxide as considerable scale/metal separation had occurred as seen in Figure 38 which shows the metal substrate from which the oxide has been pulled. The large fraction of smooth surface represents areas which were not in contact with the scale at temperature. Figure 38b also indicates that failure occurred in some contact areas by fracture within the oxide and in others by pulling oxide grains from the substrate leaving imprints behind.

The NiCoCrAlY specimens oxidized for times up to 110 hours at 1150°C formed thin Al_2O_3 scales which were too adherent to be pulled from the substrate. However, specimens oxidized for times in excess of 200 hours formed scales which spalled from about 10% of the surface during cooling. About half of the remaining oxide could be pulled from the surface while the other half remained tightly adherent. Figure 39 shows a NiCoCrAlY substrate. The dark gray areas are adherent oxide and the black areas are adhesive. These results indicate that adherence is not uniform over the surface. Study is continuing to determine what factors (e.g. distribution of the oxygen active elements etc.) are responsible for this nonuniformity.

The oxides formed on the Ni-18 Cr-6 Al-1 Hf spalled too severely on cooling from 1150°C to allow the scale-pulling tests to be performed.

The above preliminary results indicate some potential for this type of test to provide information regarding the degree of adherence of oxide scales. There are a number of experimental problems. The most important being failure of the adhesive, but work is continuing to refine the experiment.

2. Acoustic Emission Studies of Oxide Cracking

The stresses generated during the isothermal oxidation of alloys and during cooling of an oxidized alloy can result in a number of phenomena such as oxide cracking, separation between metal and oxide, and plastic deformation of either the oxide or alloy. These phenomena all give rise to acoustic emissions which, if detected and analyzed, can give information as to the physical processes involved. An acoustic emission detection system has been purchased and is currently being adapted to monitor emission both during isothermal oxidation and udring thermal cycling of the alloys being studied. Figure 40 shows an example of acoustic emissions produced by the isothermal oxidation of Nb^5. It is seen that there are no emissions during the initial stages of oxidation. Weight change data, also plotted in Figure 40, indicate a decreasing oxidation rate during this period. Rapid scale cracking is indicated by acoustic emission to begin after about 10 minutes and the oxidation rate becomes linear at this time. The linear rate is believed due to the cracks forming parallel to the specimen surface which keep the oxide diffusion barrier at a constant thickness.

The above example of the oxidation of Nb is a case where cracking is extensive. However, the sensitivity obtainable with modern acoustic emission is capable of detecting cracking on a much finer scale and other subtle phenomena. It is, therefore, planned to employ acoustic emission to follow both the isothermal growth of Al_2O_3 and SiO_2 and cracking due to thermal stresses. It is important to emphasize that one of the major problems in studying the adherence of α-Al_2O_3 scales on alloys has been the lack of meaningful techniques to determine and compare the scale adherence on different alloys. It is believed that the oxide stripping procedures and the use of acoustic emission may provide new, more quantitative information regarding scale cracking and should allow such variables as alloy composition, alloy surface preparation, amount and

type of oxygen active element, and alloy fabrication condition to be evaluated with regards to their effects on scale growth mechanisms and scale adherence.

SUMMARY AND CONCLUDING REMARKS

During the second year of this program the development of silicon - containing scales and α-Al_2O_3 scales on alloys has been studied. The weight change versus time data which have been obtained suggest that the silicon - containing scales may be comparable to α-Al_2O_3 as a means of developing high temperature oxidation resistance. The silicon - containing scales, however, have been observed to be developed along with substantial amounts of transient oxidation. In addition, the results suggest that nickel may diffuse through the silicon scales. Both of these conditions are undesirable freatures in regards to using such scales as barriers to inhibit oxidation. During the third year of this program work must be directed towards:

1. Determining if relatively pure SiO_2 scales can be developed on nickel- and cobalt- base alloys at silicon concentrations which are realistic for use in coatings.
2. The rate constants for the growth of these scales must be obtained and compared to those for α-Al_2O_3.
3. The long term stability of these scales must be evaluated as well as the ability of these scales to be reformed after cracking and spalling of the first-formed scale.
4. Providing silica scales are formed which grow at sufficiently slow rates and these scales are stable over long exposure times (e.g. $\sim$1000 hrs. at 1100°C), the adherence of the scales will then be examined.

The oxide scale stripping test and the use of acoustic emission to detect oxide scale cracking and spalling should provide more quantitative means to examine

the factors which affect oxide scale adherence. The results obtained to date show that the condition of the surfaces of coatings are critical to α-Al_2O_3 scale development and adherence. Experiments will now be performed to attempt to accomplish the following:

1. Compare α-Al_2O_3 Scale Adherence as a function of
   -different concentrations of the same oxygen active elements (e.g. Y, Hf)
   -the same concentrations of two different elements
   -the effects of using two oxygen active elements (Y + Hf)
   -the same concentration of the same oxygen active element but with the element in the alloy in the unoxidized and oxidized states.
   -first formed and second formed α-Al_2O_3 scales.
2. Analysis of the factors that lead to spalling of α-Al_2O_3 scales, including
   -the relative importance of growth and thermally-induced stresses.
   -the importance of the mechanism by which the α-Al_2O_3 is formed.
3. Characterization and documentation of the structural features of α-Al_2O_3 scales,
   -what is a typical structure
   -how does structure vary in regards to substrate structure
   -how critical is oxide structure to oxide scale growth rate.
   -how critical is oxide structure to oxide scale adhesion.
   -can oxide scale structure ever be effectively controlled.

As the results become available from the experiments involving the silicon - containing scales, it will become apparent if studies on the adhesion of these scales using the techniques developed with the α-Al_2O_3 scales should be performed.

REFERENCES

1. G. H. Meier and F. S. Pettit, "Fundamental Research Directed To Advanced High Temperature Coating Systems Beyond The Current State-Of-The-Art Systems", University of Pittsburgh, First Annual Report on AFOSR Contract No. AFOSR-80-0089, April 15, 1981.

2. F. S. Pettit, Trans. A.I.M.E., 239, 1296 (1967).

3. C. Wagner, J. Appl. Phys. 29, 1295 (1958).

4. R. N. Ghoshtagore, J. Appl. Phys., 40, 4374 (1969).

5. R. A. Perkins and G. H. Meier, unpublished research.

ACKNOWLEDGMENT

The authors express their appreciation to Dr. Susan Wood of Westinghouse Research and Development Center for preparing the ion implanted specimens used in this study.

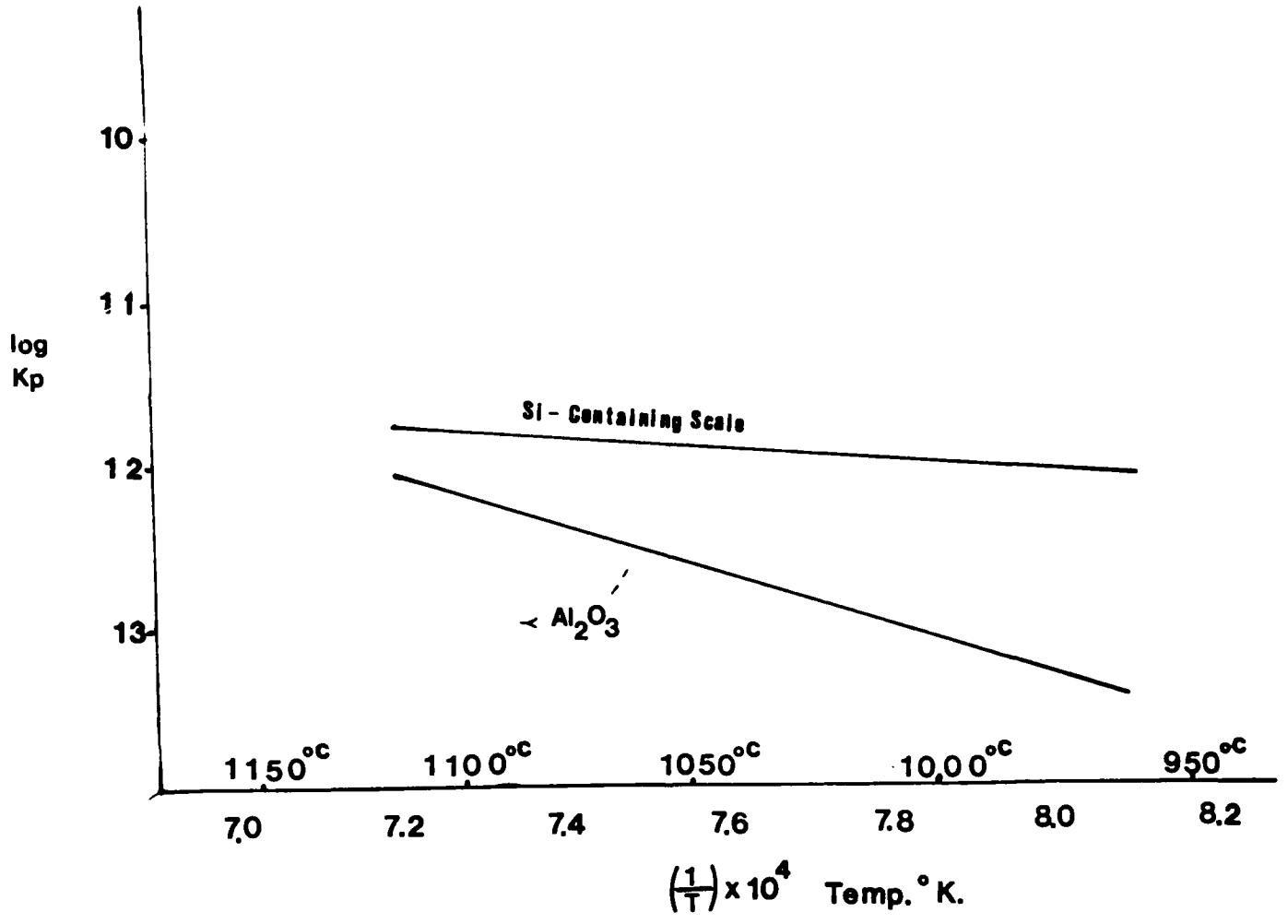

Figure 1. Comparison of parabolic rate constants for oxidation of Ni-7.5 Si alloys and Al_2O_3 - growth.

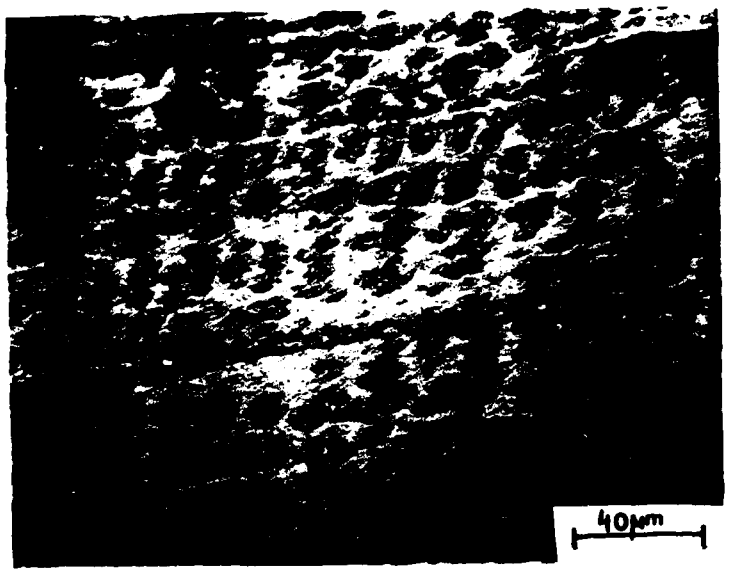

Figure 2. Scale/gas interface of Ni-7.5 Si oxidized for 20 hours at 950°C in oxygen.

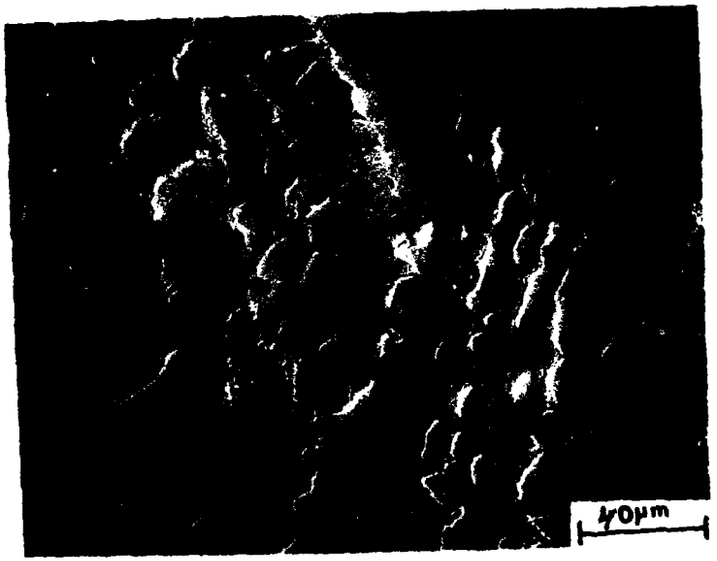

Figure 3. Cast structure of Ni-7.5 Si substrate.

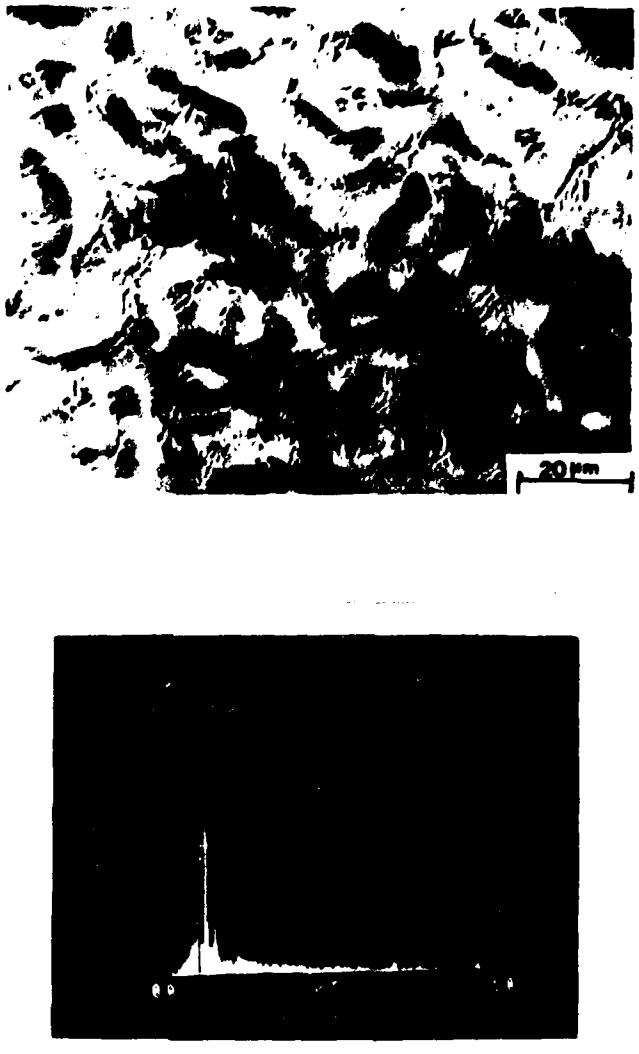

Figure 4. Alloy side of oxide formed on Ni-7.5 Si at 950°C and corresponding EDAX spectrum indicating only Si.

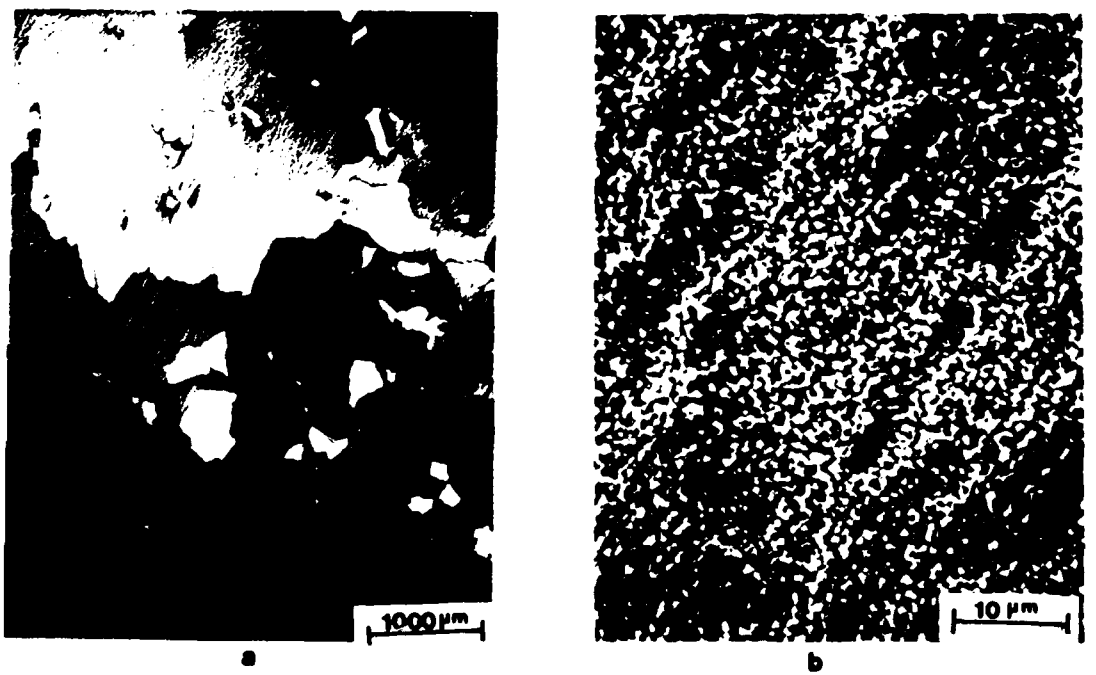

Figure 5. Scale/gas interface of Ni-7.5 Si oxidized for 72 hours at 950°C in oxygen (a,b,c) and EDAX spectrum of oxide crystals (d).

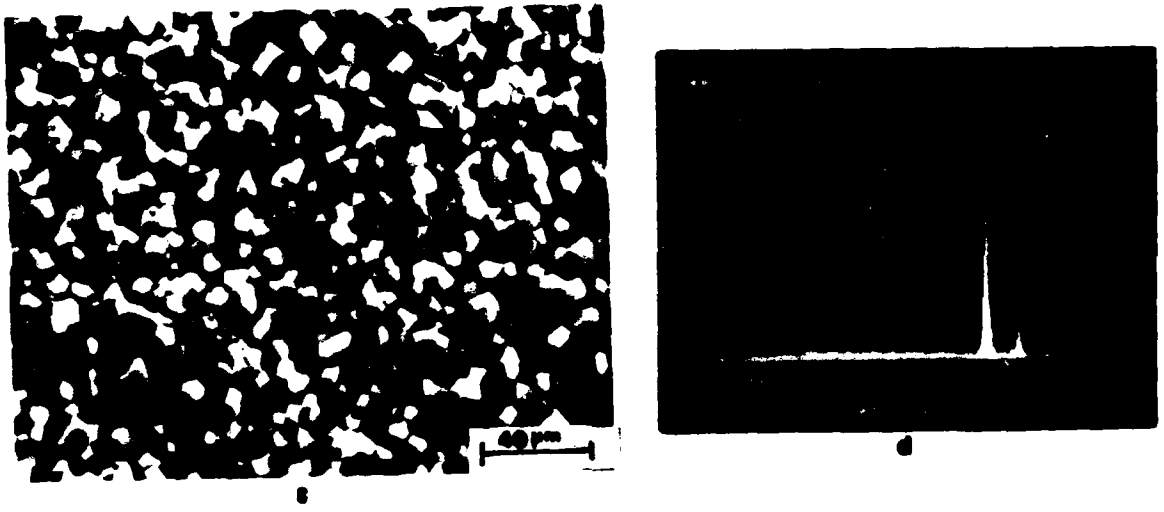

Figure 5. (Continued)

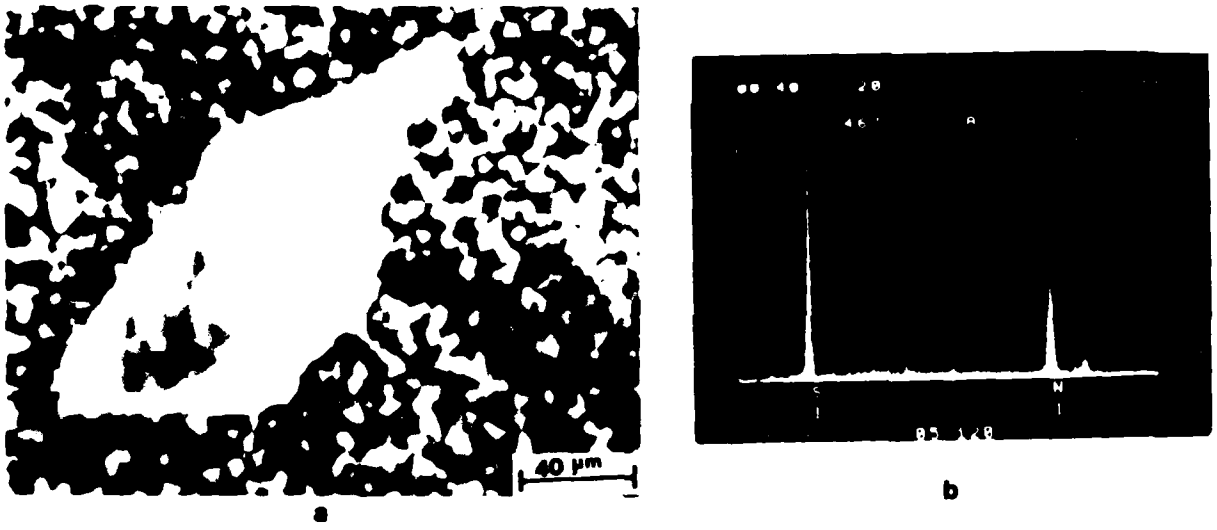

Figure 6. Spalled oxide flake on Ni-7.5 Si oxidized for 72 hours at 950°C (a) and corresponding EDAX spectrum (b).

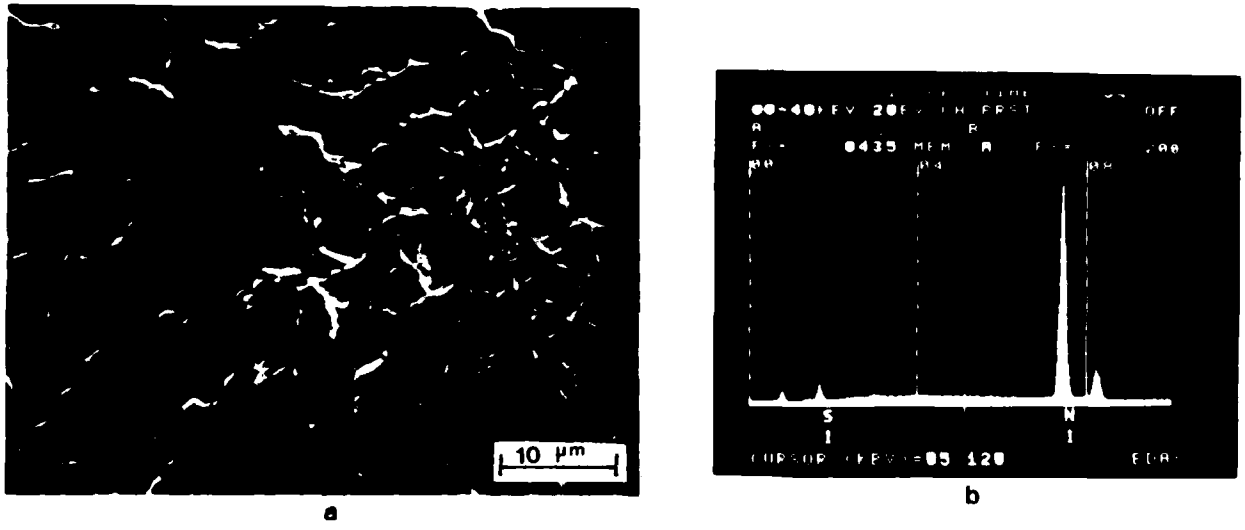

Figure 7. Substrate for Ni-7.5 Si from which the scale has spalled on cooling after oxidation for 72 hours at 950°C (a) and corresponding EDAX spectrum (b).

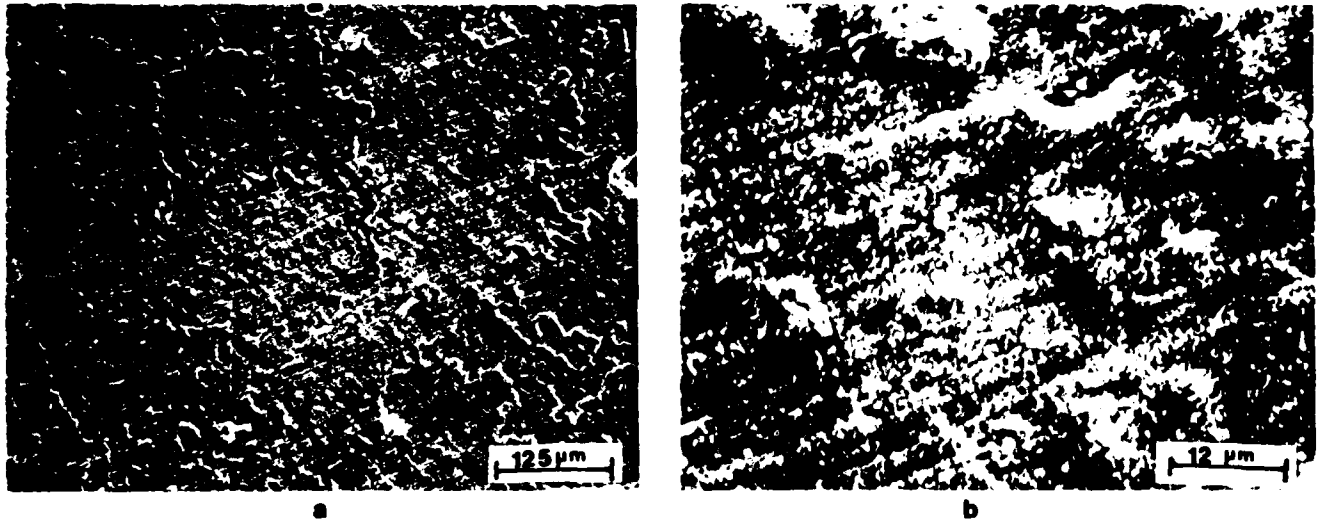

Figure 8. Scale/gas interface of Ni-7.5 Si oxidized for 48 hours at 1000°C in argon containing O_2 impurities ($P_{O_2} \simeq 10^{-6}$-10^{-5} atm.) (a,b,c) and corresponding EDAX spectrum (d).[2]

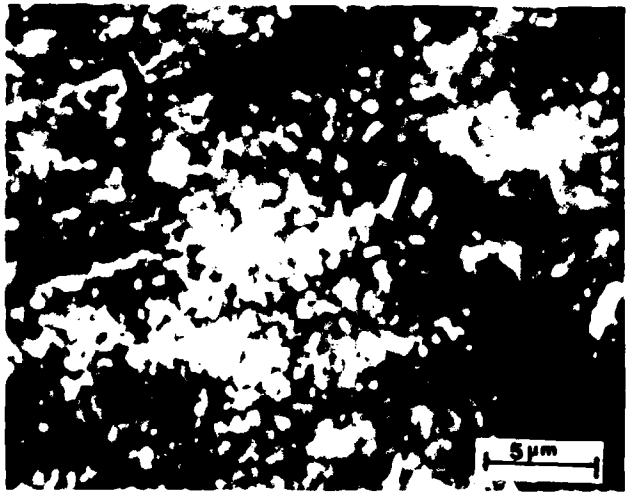

c

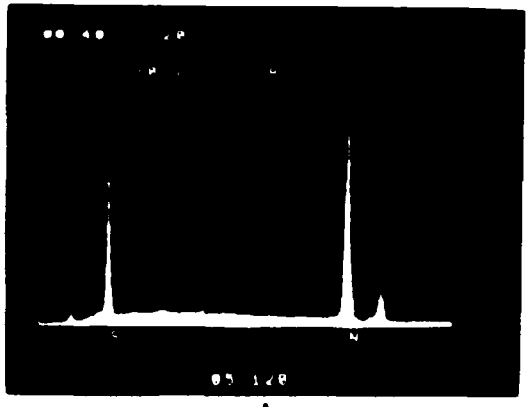

d

Figure 8. (Continued)

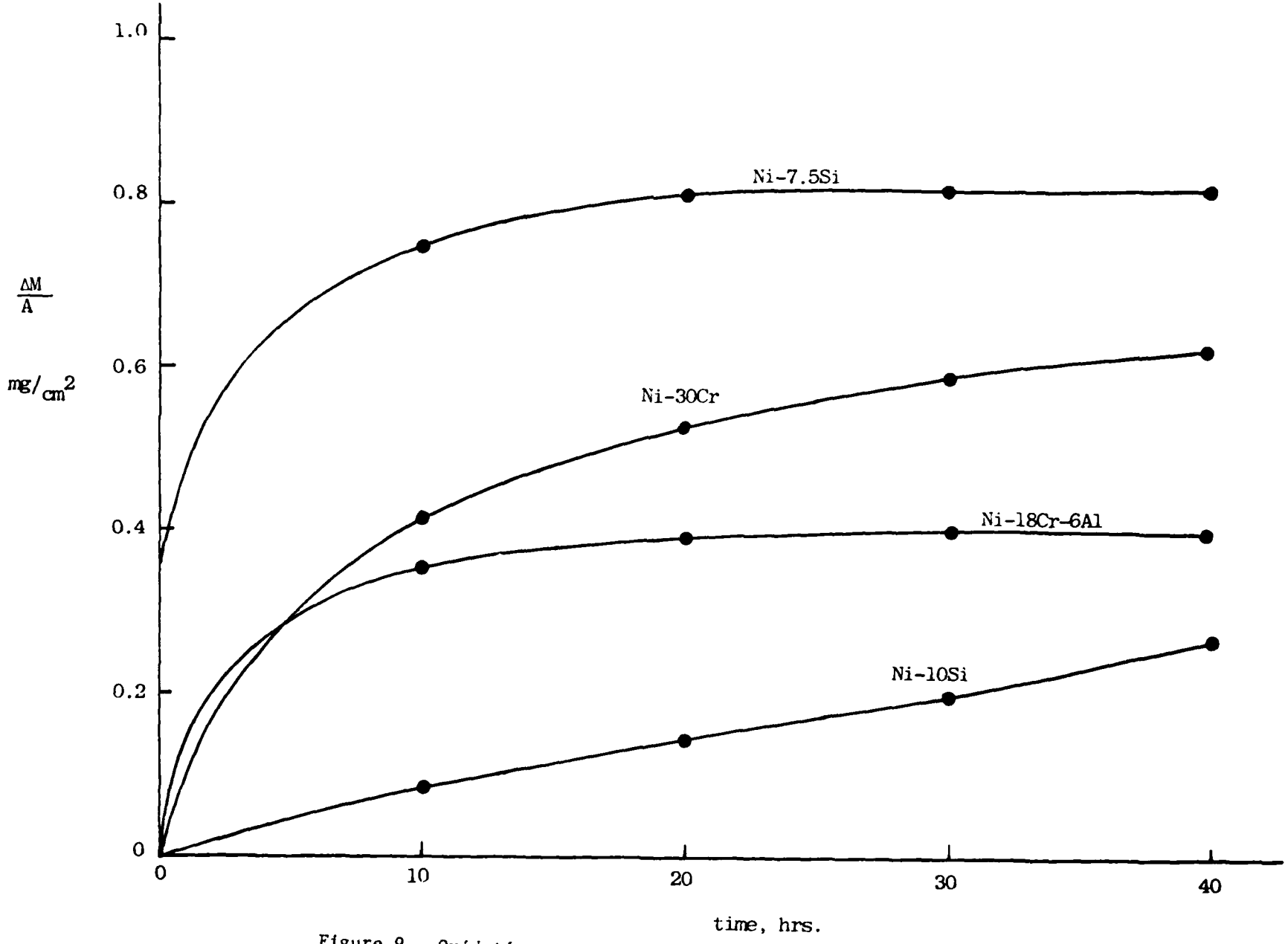

Figure 9. Oxidation rates of Ni-10 Si at 1000°C and Ni-7.5 Si, Ni-30 Cr, and Ni-18 Cr-6 Al at 950°C.

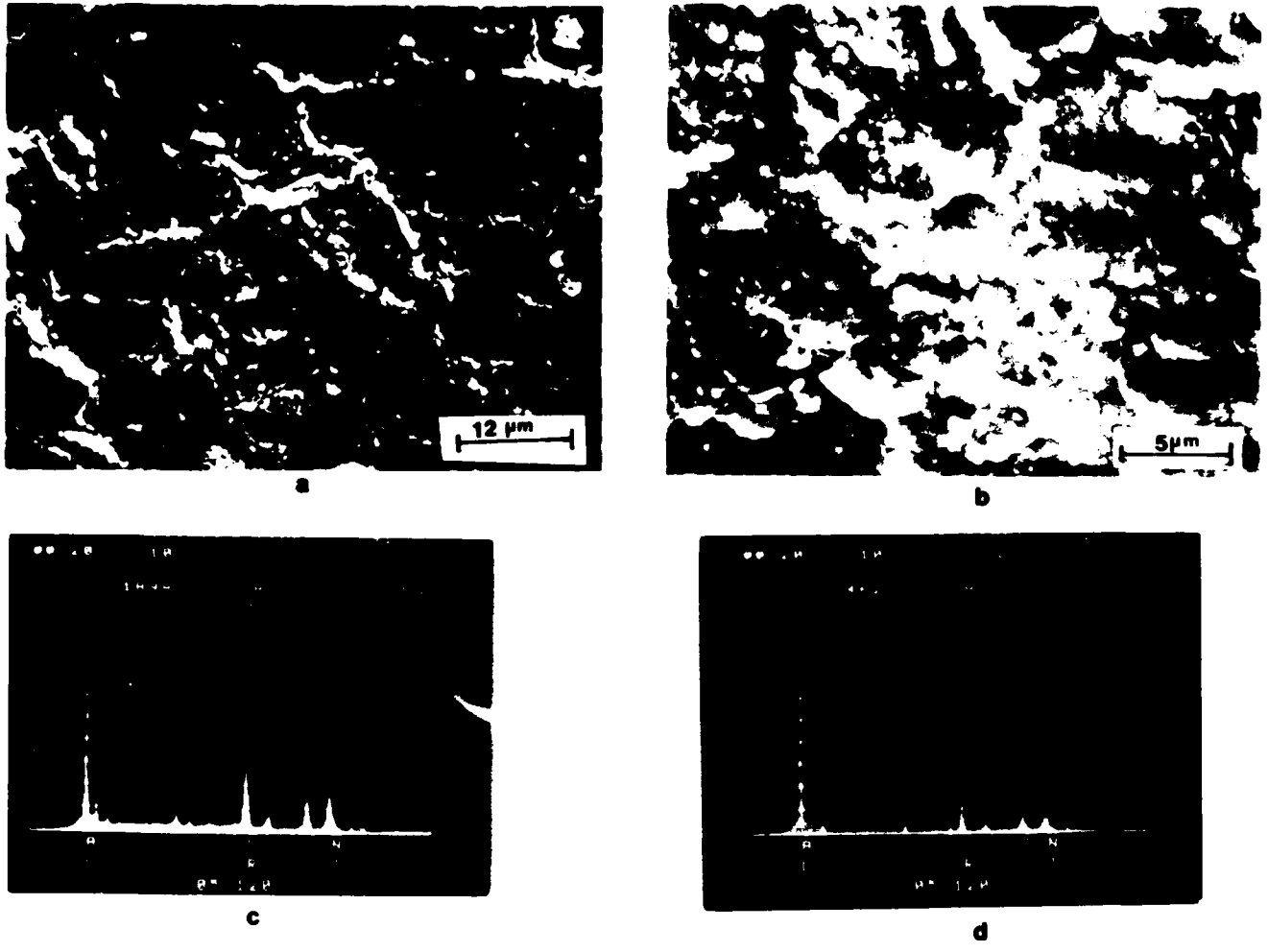

Figure 10. Scale/gas interface of as-processed, plasma-sprayed NiCoCrAlY oxidized for 1 hour at 1100°C (a,b), EDAX spectrum of entire surface (e) and EDAX spectrum of white particles in 10b (d).

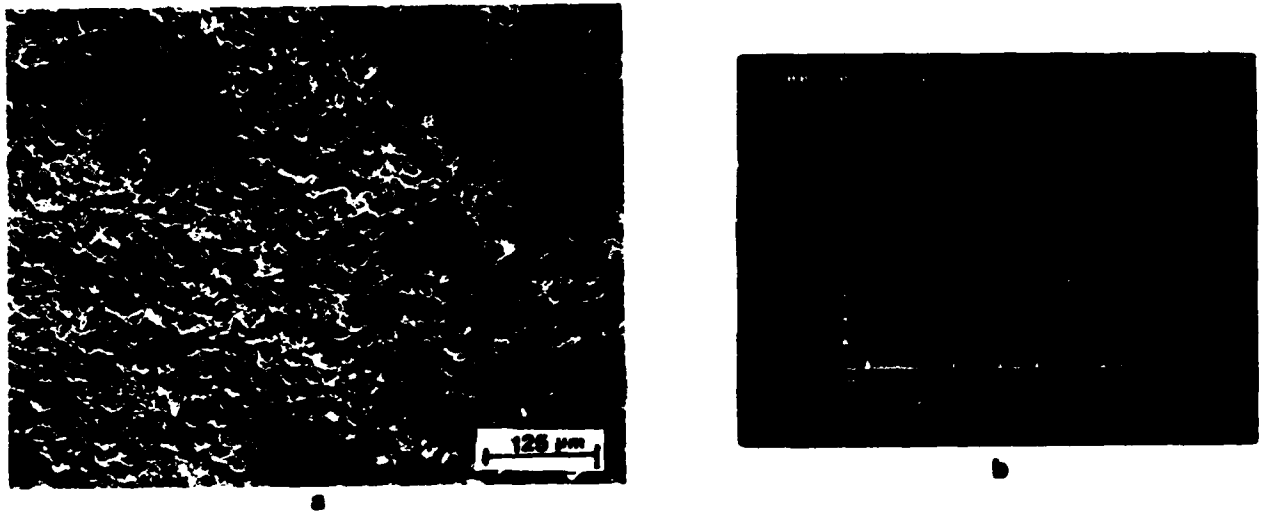

Figure 11. Scale/gas interface of as-processed, plasma sprayed NiCoCrAlY oxidized for 24 hours at 1100°C (a) and corresponding EDAX spectrum (b).

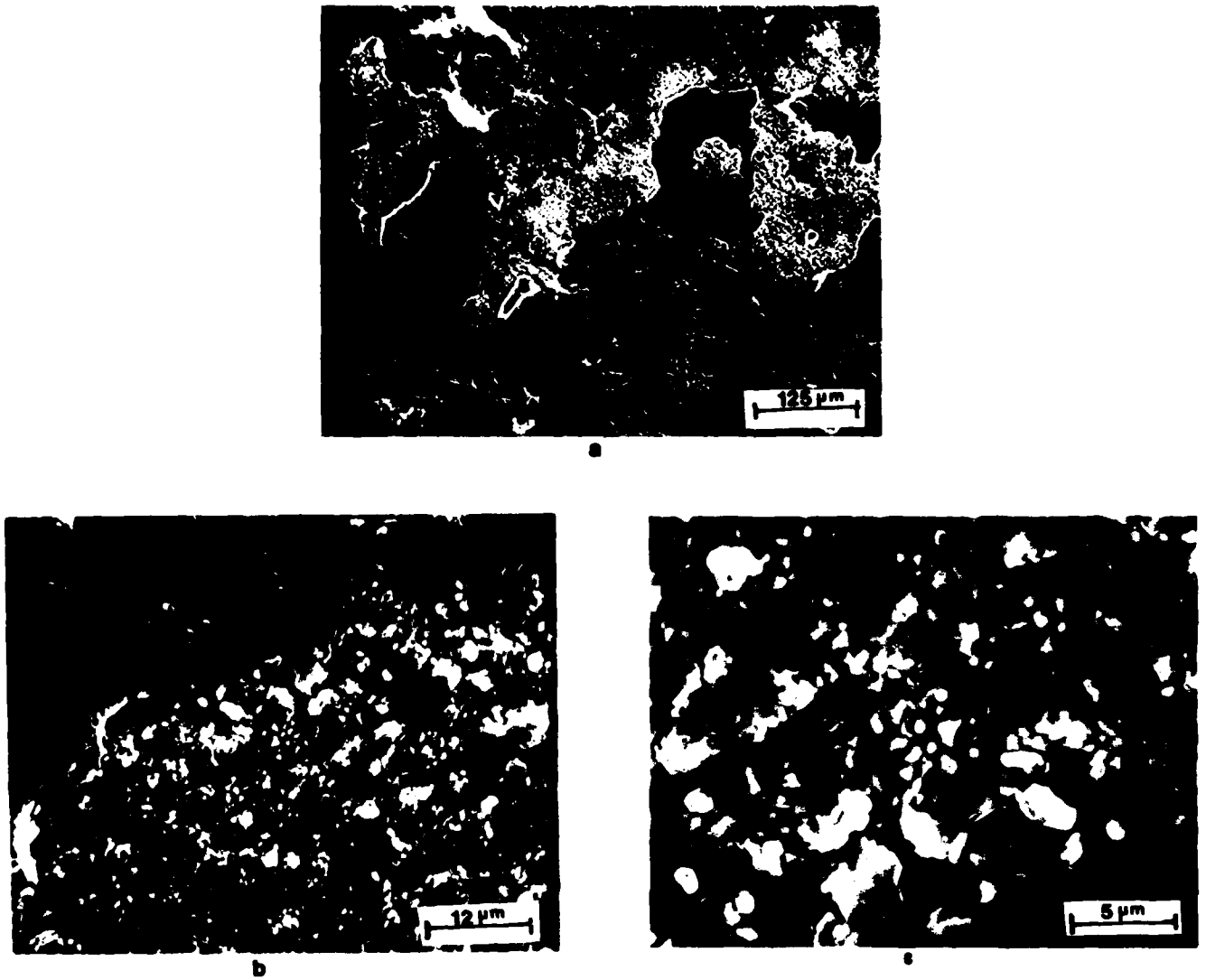

Figure 12. Scale/gas interface of polished, plasma-sprayed NiCoCrAlY oxidized for 1 hour at 1100°C also showing substrate from which the scale has spalled on cooling.

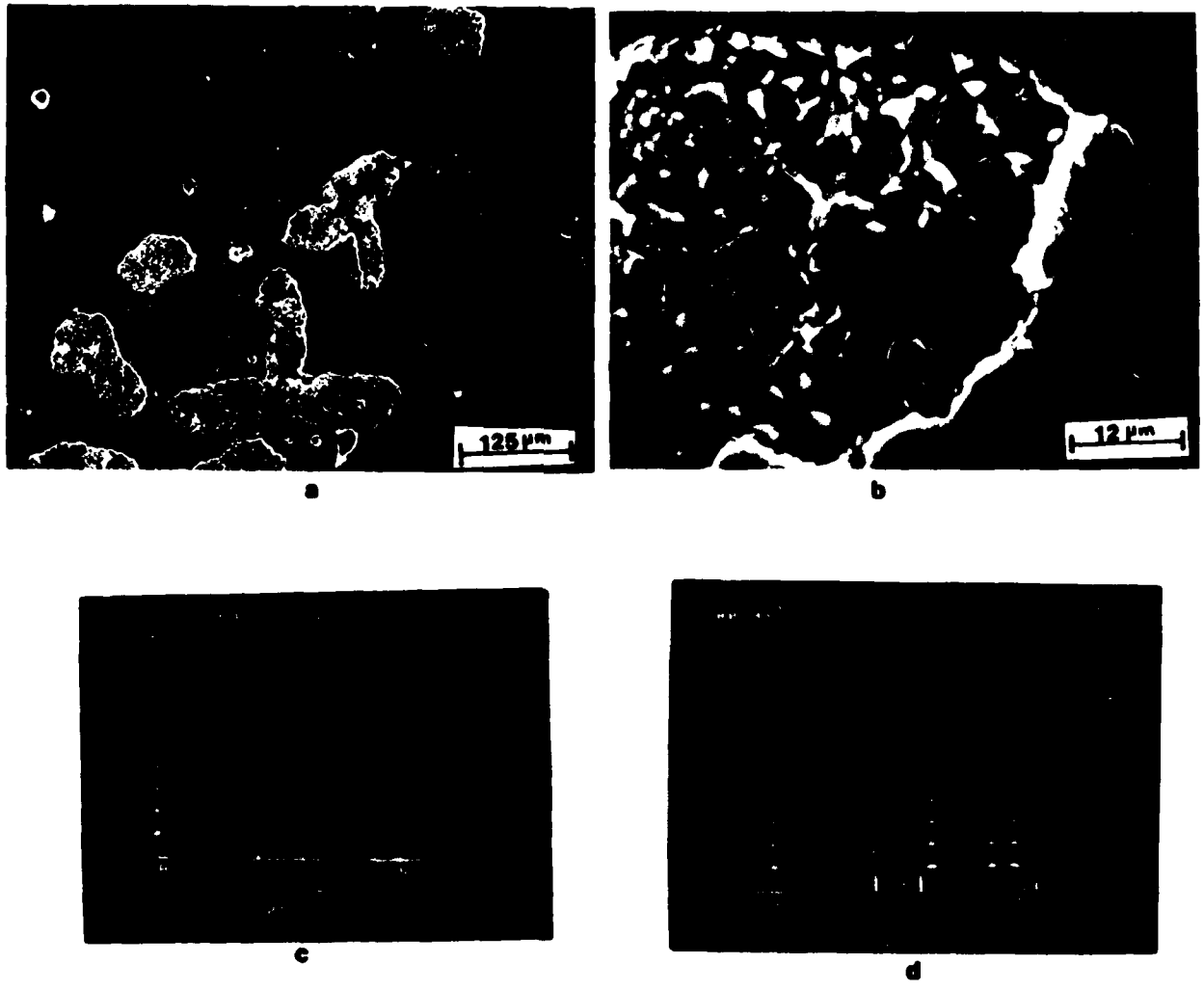

Figure 13. Scale/gas interface of polished, plasma-sprayed NiCoCrAlY oxidized for 24 hours at 1100°C (a,b) and EDAX spectra of scale (e) and substrate (d).

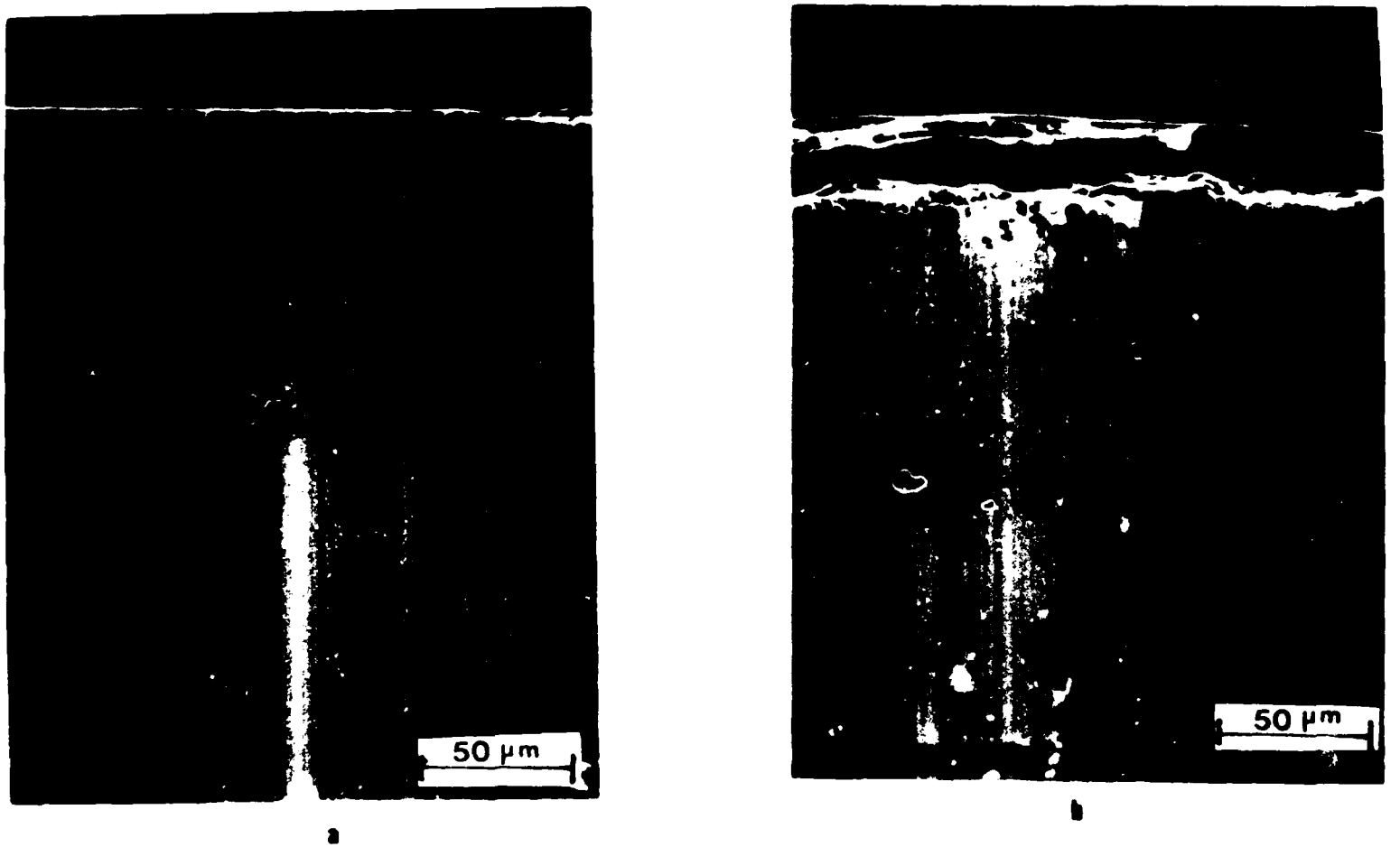

Figure 14. Cross-section of NiCoCrAlY coatings from Figure 13 and 11. Polished side (a) and as-processed side (b).

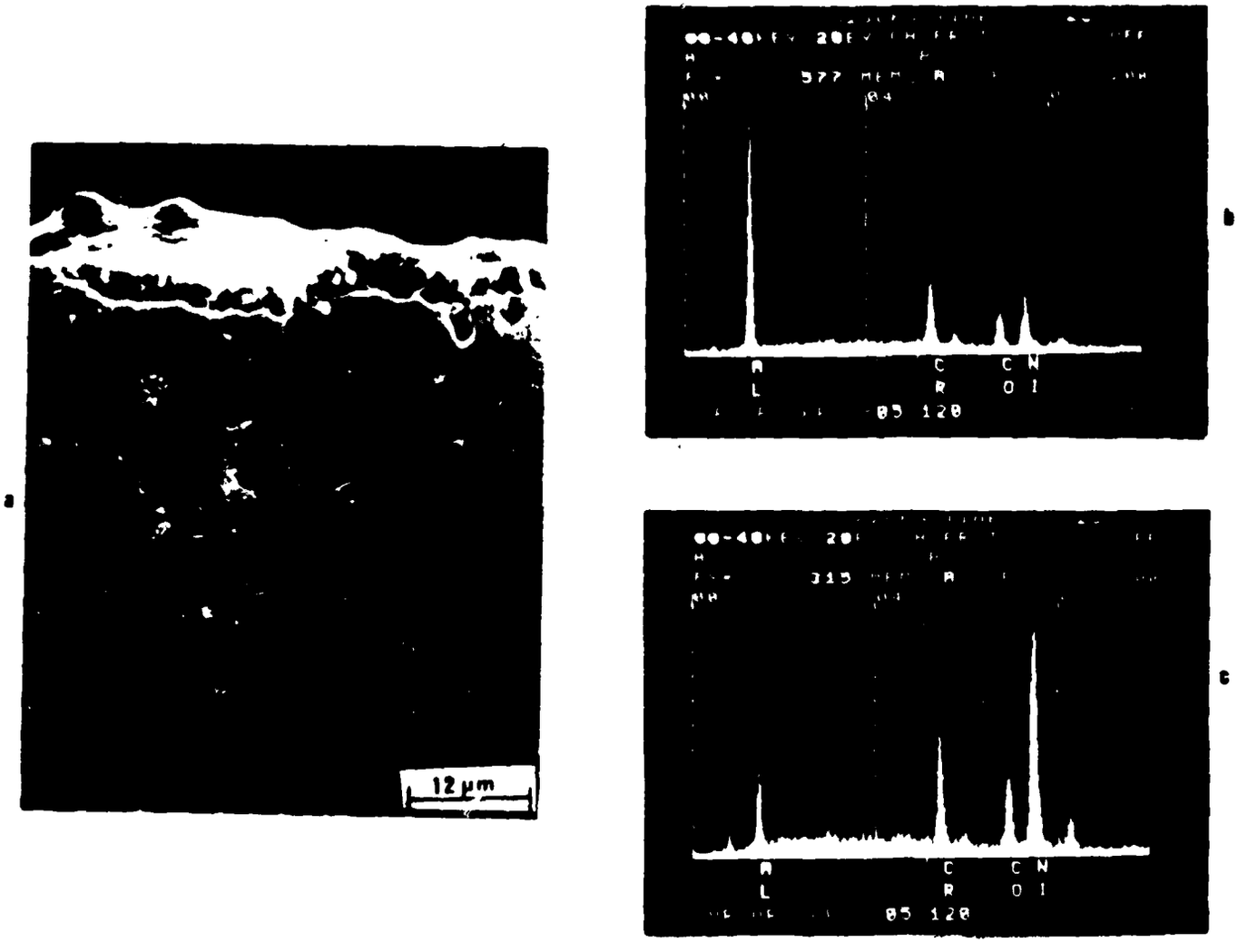

Figure 15. Cross-section of as-processed, plasma-sprayed NiCoCrAlY oxidized for 24 hours at 1100°C (a) and EDAX spectra of dark oxide (b) and matrix around the dark oxide (c).

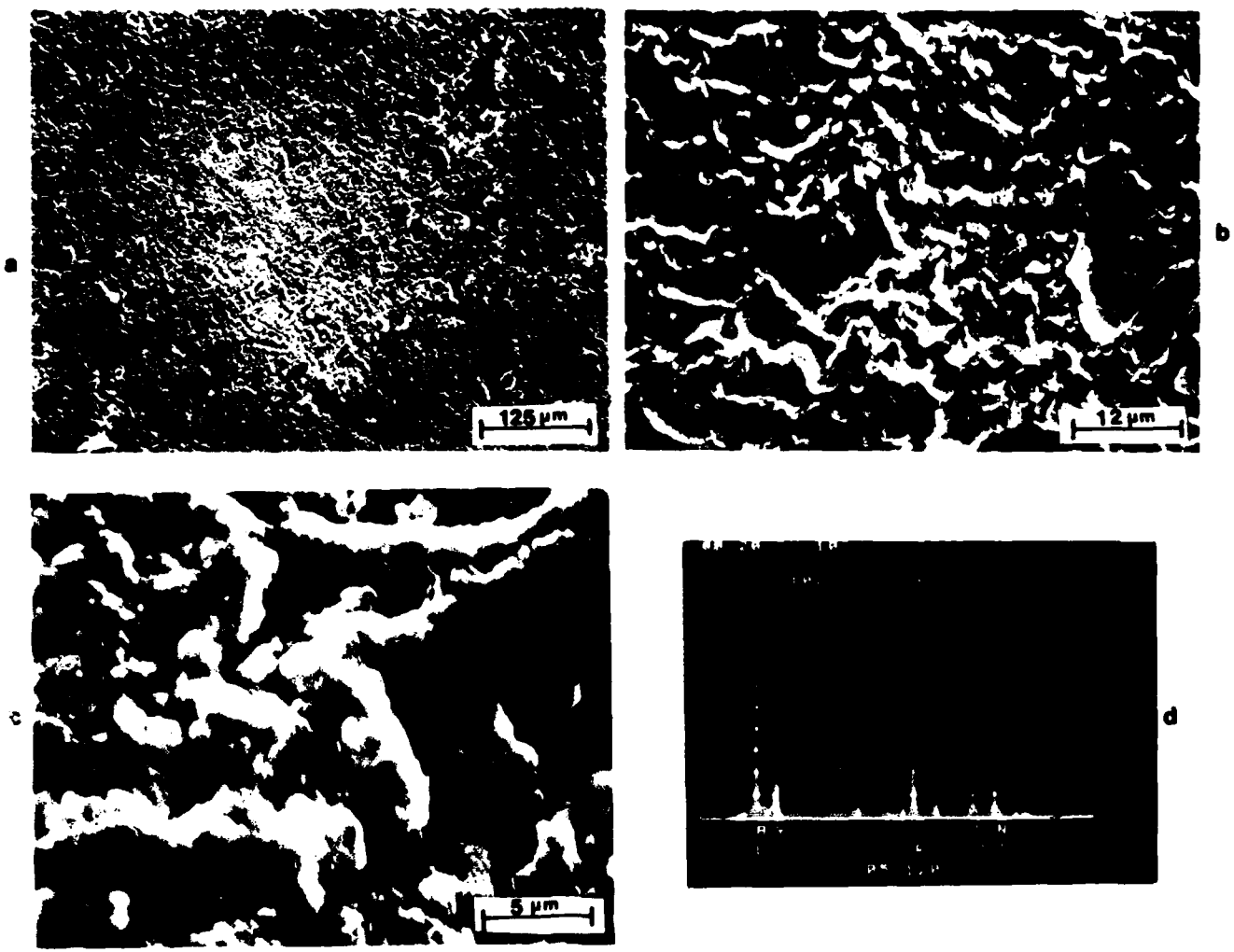

Figure 16. Scale/gas interface of as-processed, PVD NiCoCrAlY oxidized for 1 hour at 1100°C (a,b,c) and EDAX spectrum of the surface (d).

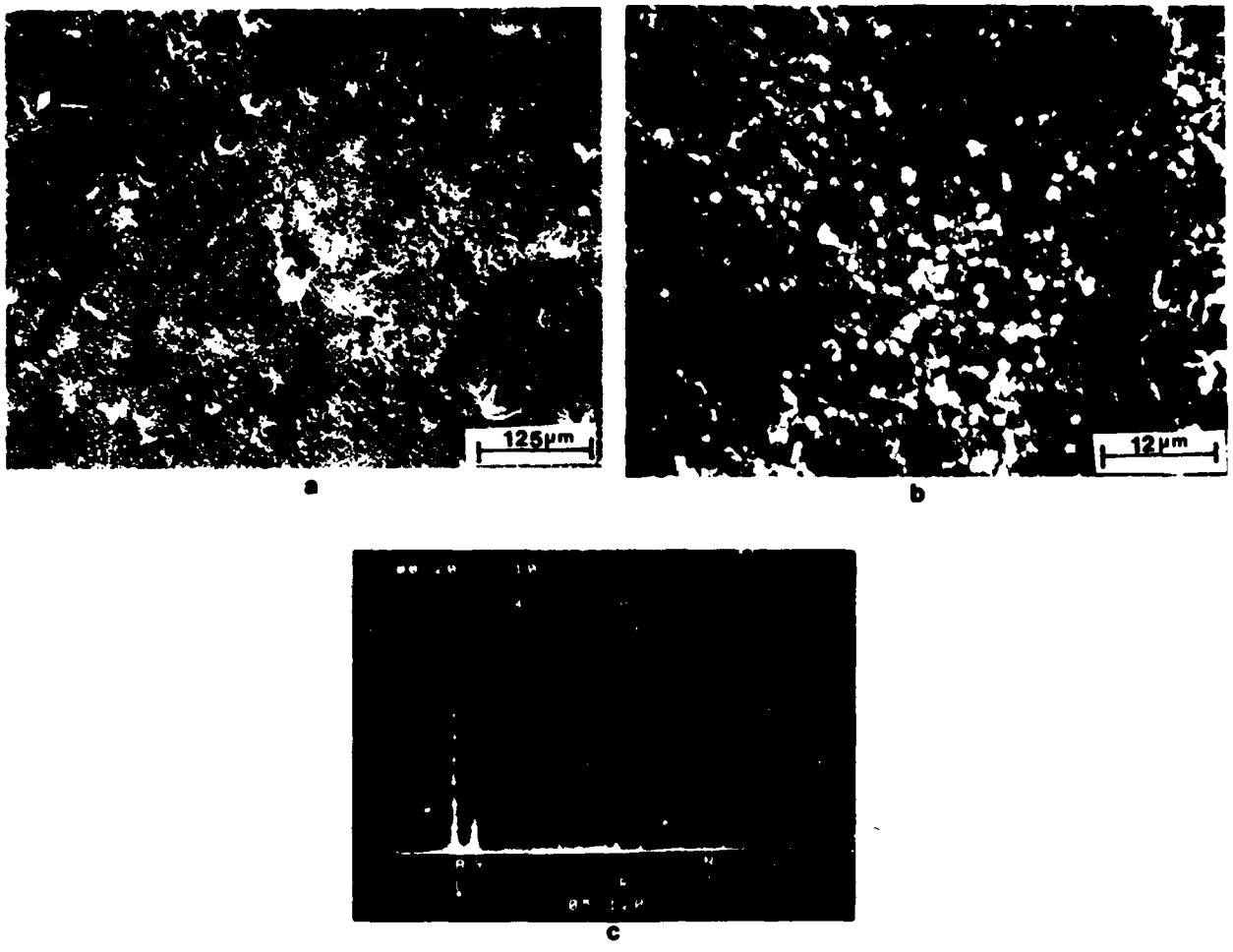

Figure 17. Scale/gas interface of as-processed, PVD NiCoCrAlY oxidized for 24 hours at 1100°C (a,b) and EDAX spectrum of the surface (c).

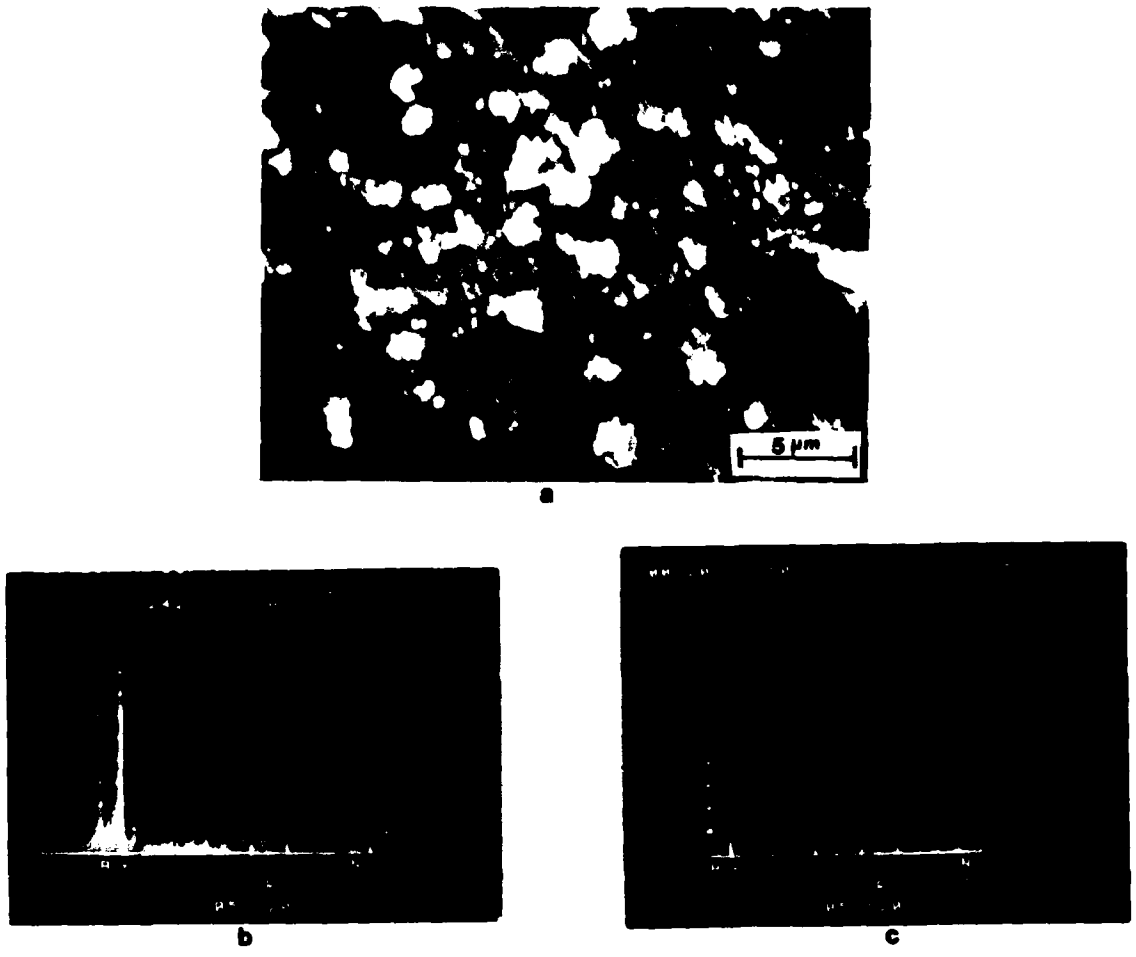

Figure 18. Scale/gas interface of as-processed, PVD NiCoCrAlY oxidized for 24 hours as 1100°C (a) and EDAX spectra of the white particles (b) and areas between the particles (c).

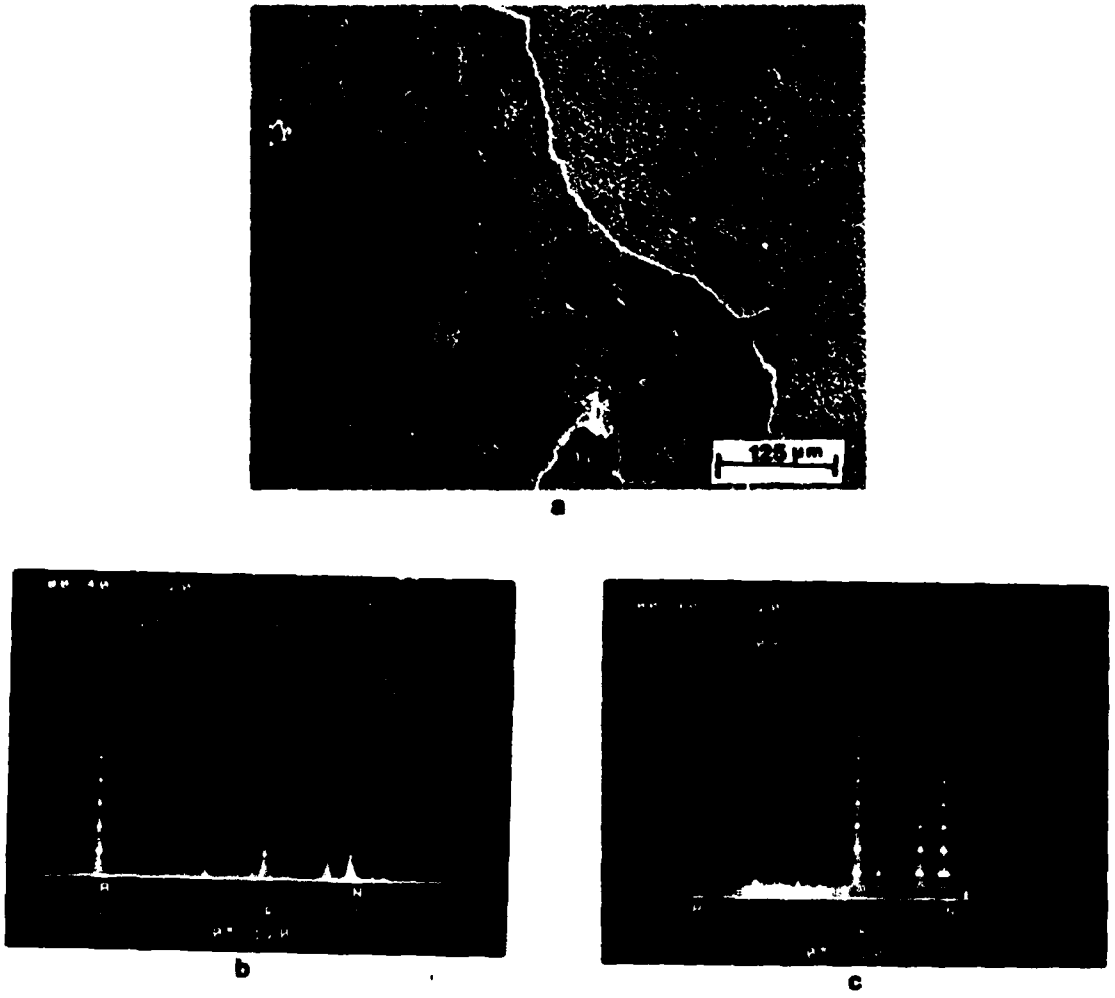

Figure 19. Scale/gas interface of polished, PVD NiCoCrAlY oxidized for 1 hour at 1100°C (a) and EDAX spectra of the scale (b) and the alloy substrate (c).

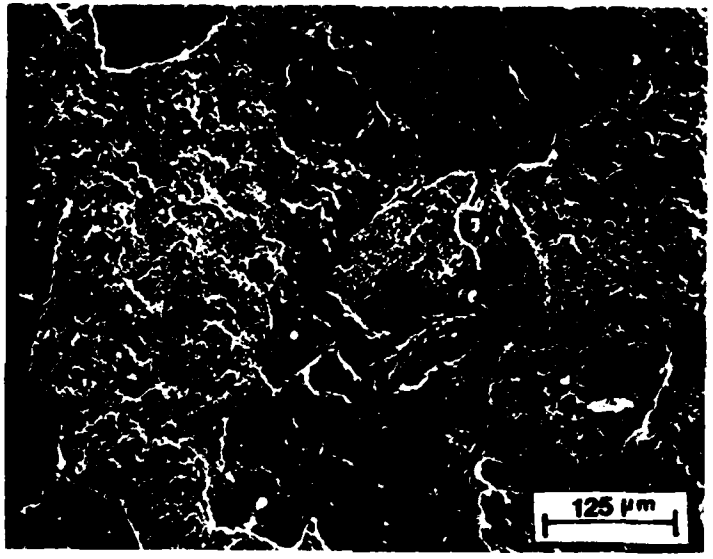

Figure 20. Scale/gas interface of polished, PVD NiCoCrAlY oxidized for 24 hours at 1100°C (a), the substrate from which the scale has spalled (b) and EDAX spectra of the scale (c) and substrate (d).

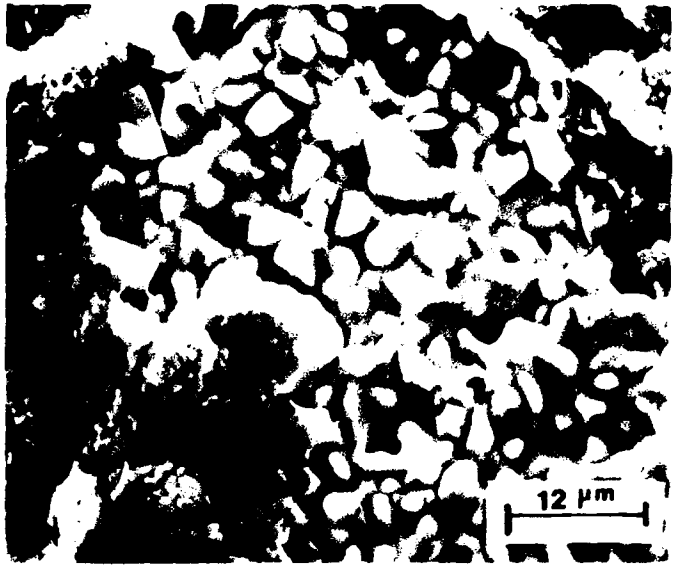

b

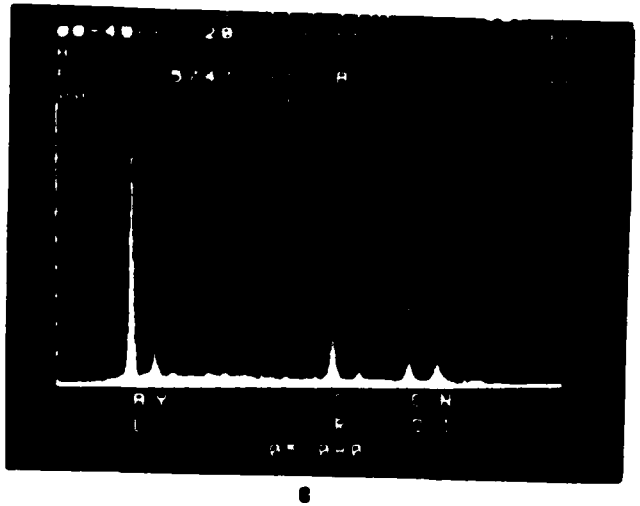

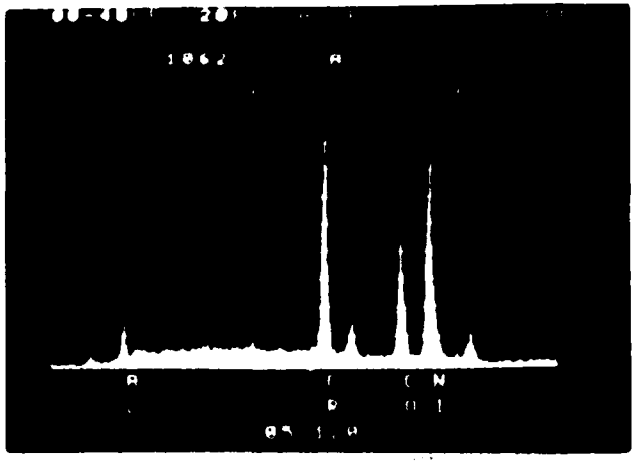

c

Figure 20. (Continued)

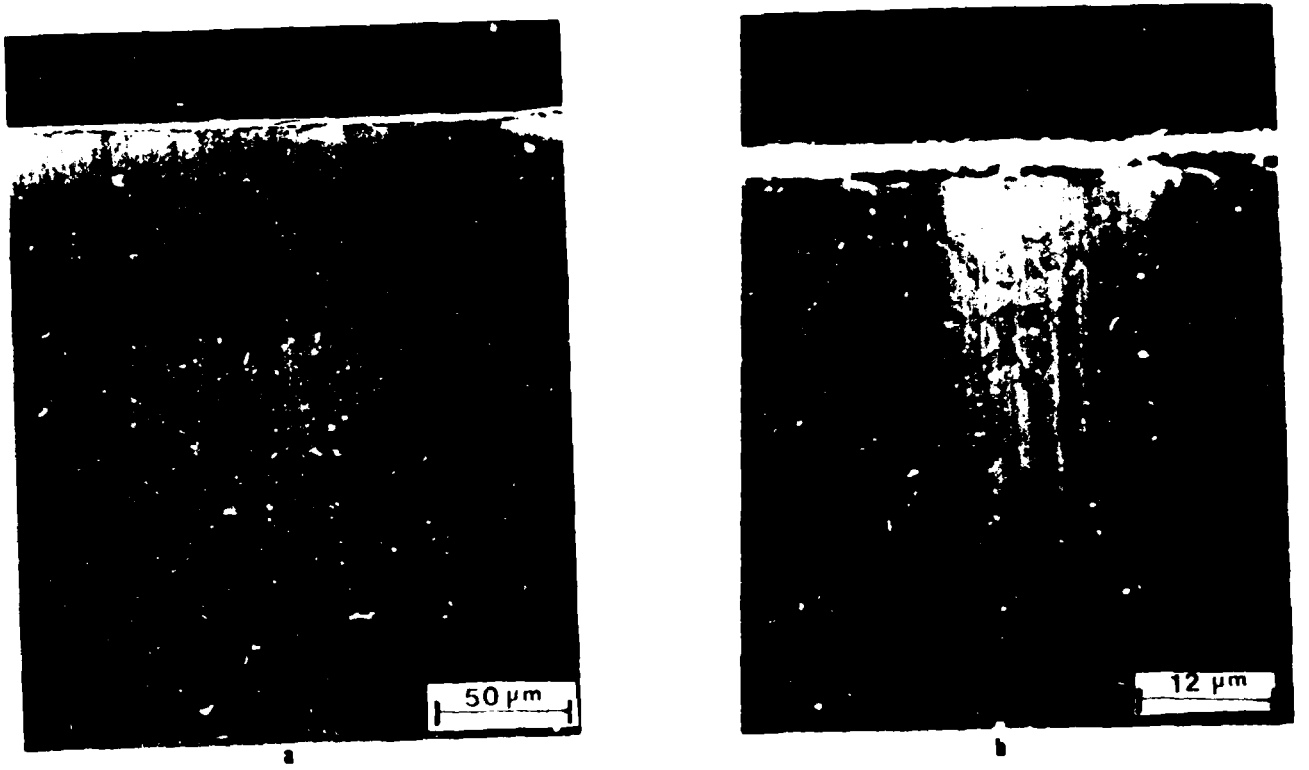

Figure 21. Cross-section of as-processed, PVD NiCoCrAlY oxidized for 24 hours at 1100°C.

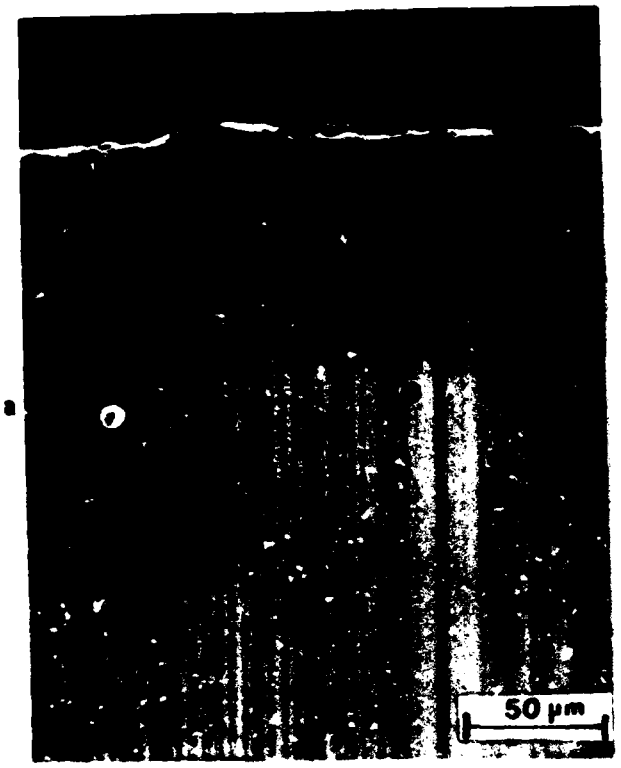

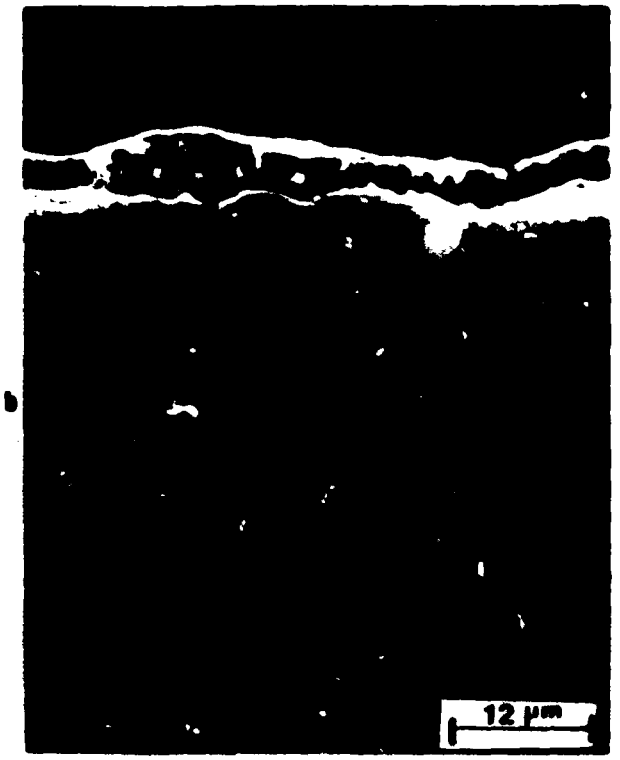

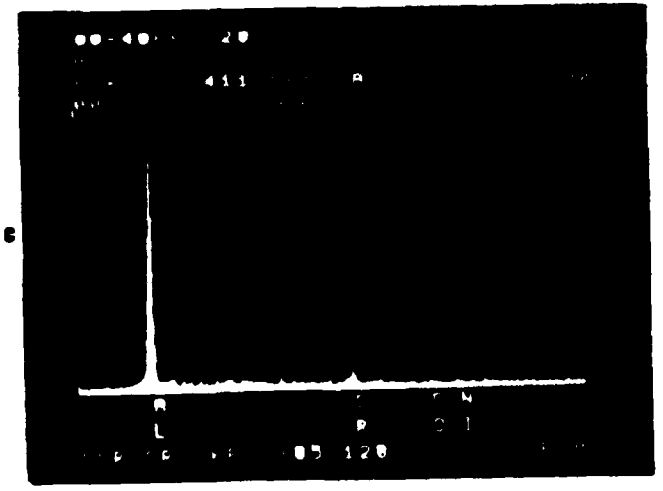

Figure 22. Cross-section of polished, PVD NiCoCrAlY oxidized for 24 hours at 1100°C (a,b) and EDAX spectrum of scale.

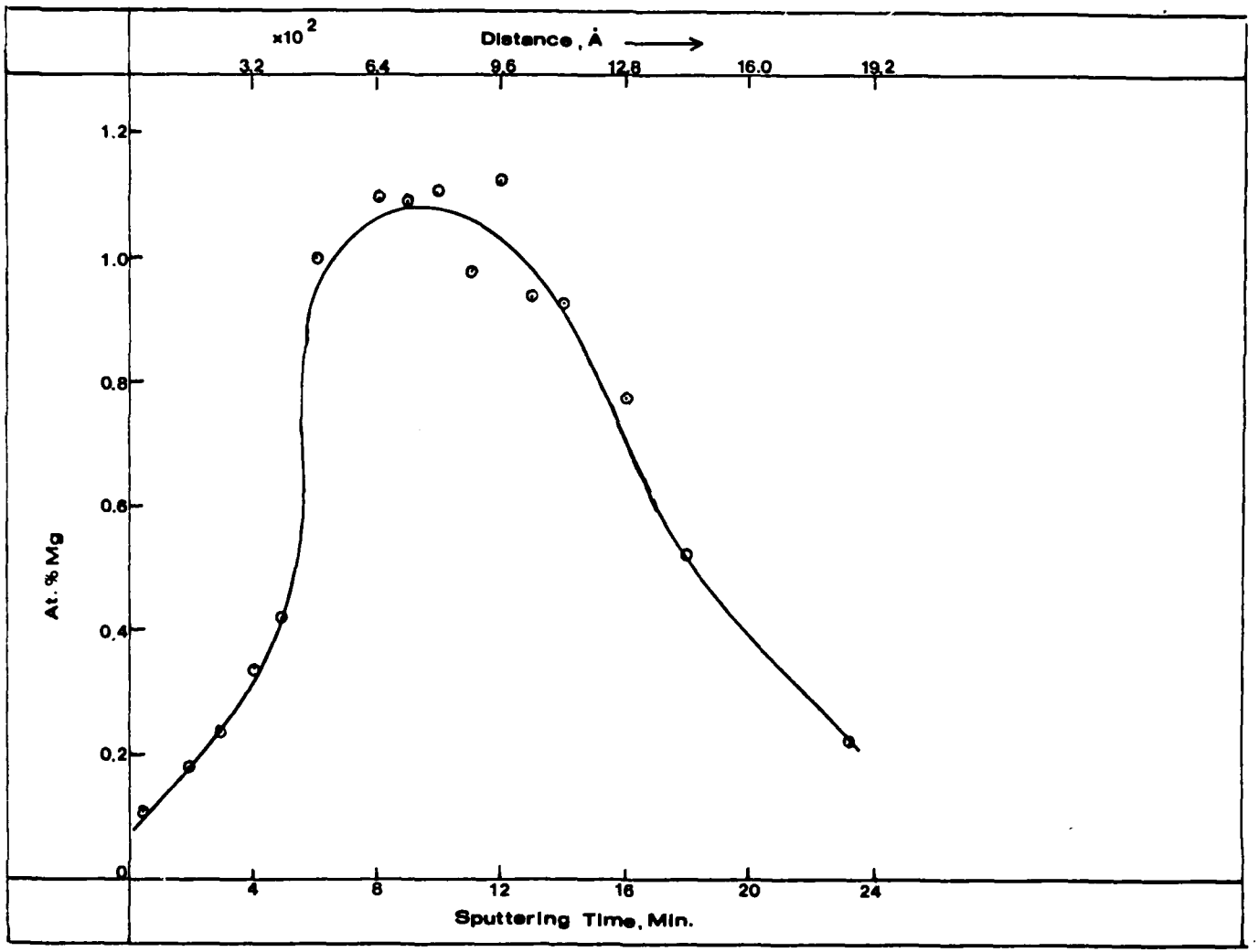

Figure 23. Concentration profile of Mg in ion-implanted Ni.

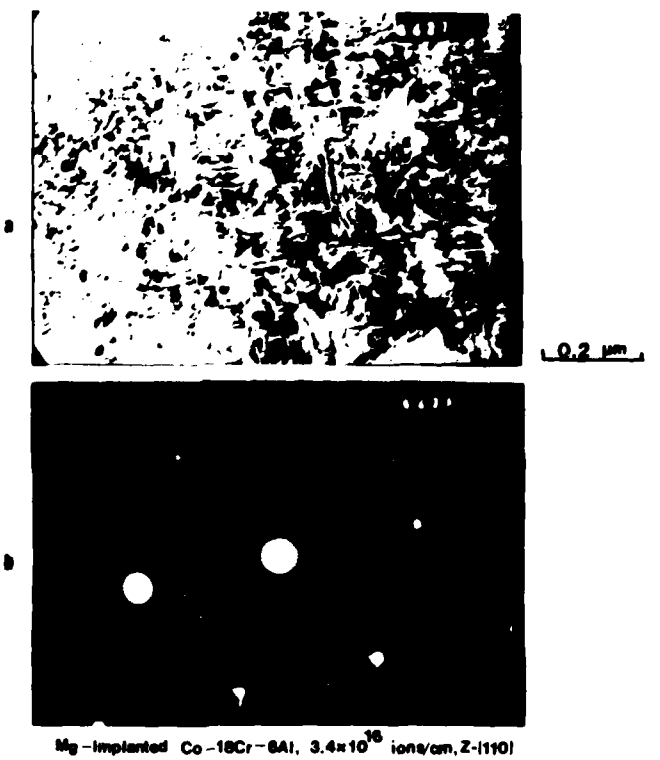

Figure 24. Transmission electron micrographs of the implanted region of Mg-implanted CoCrAl (a) and corresponding selected area diffraction pattern (b).

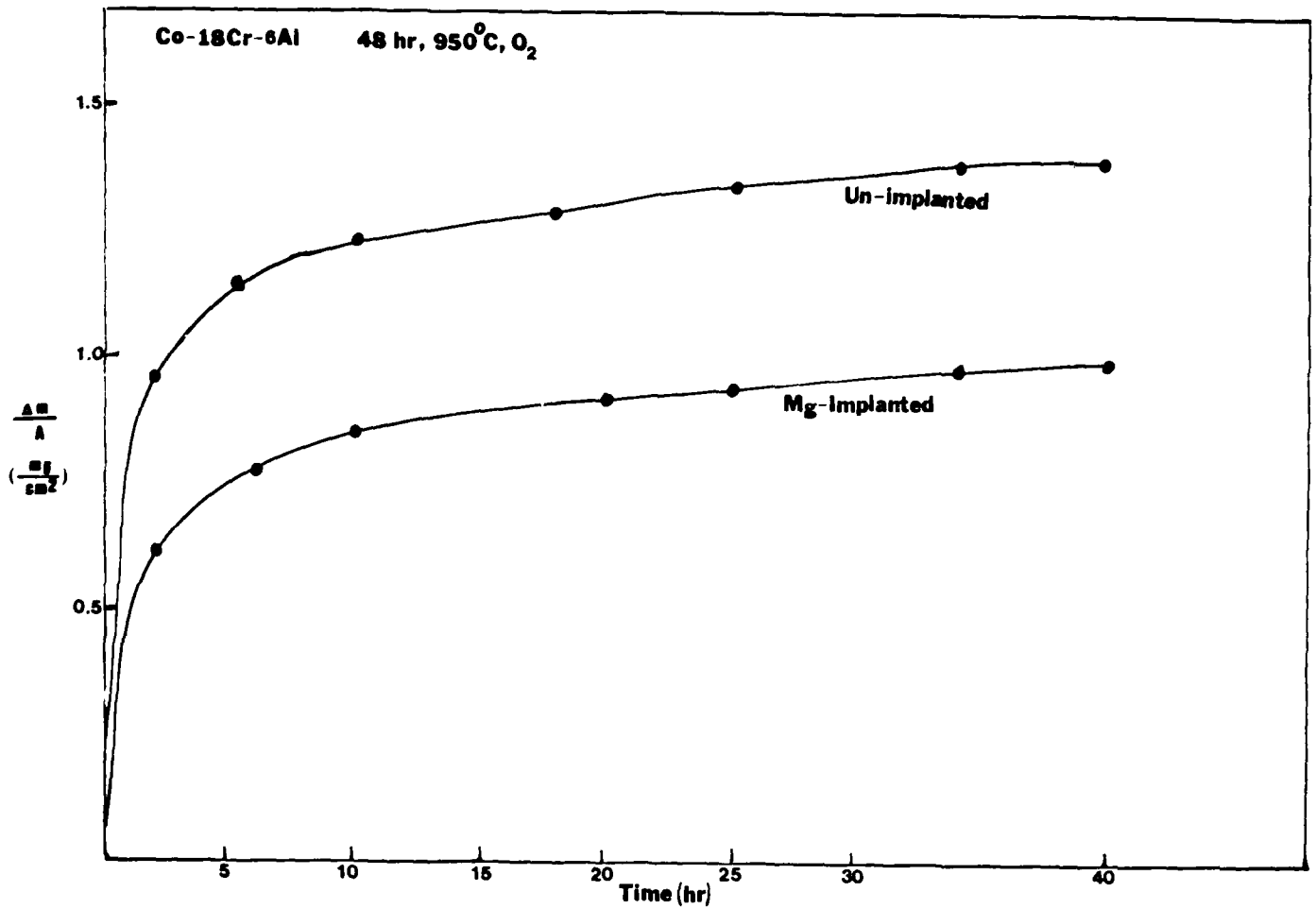

Figure 25. Oxidation rates of Co-18 Cr-6 Al and Mg-implanted Co-18 Cr-6 Al.

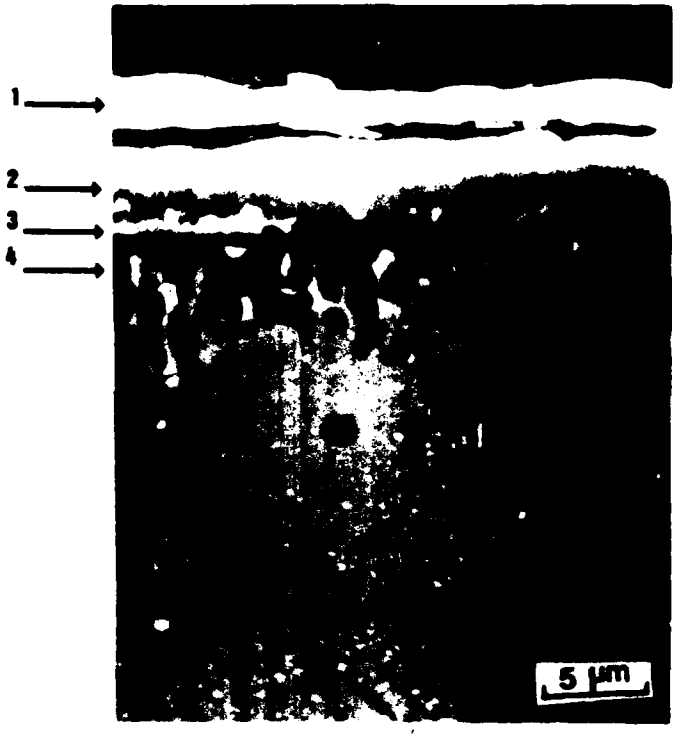

Figure 26. Cross section CoCrAl oxidized for 48 hours in oxygen at 950°C.

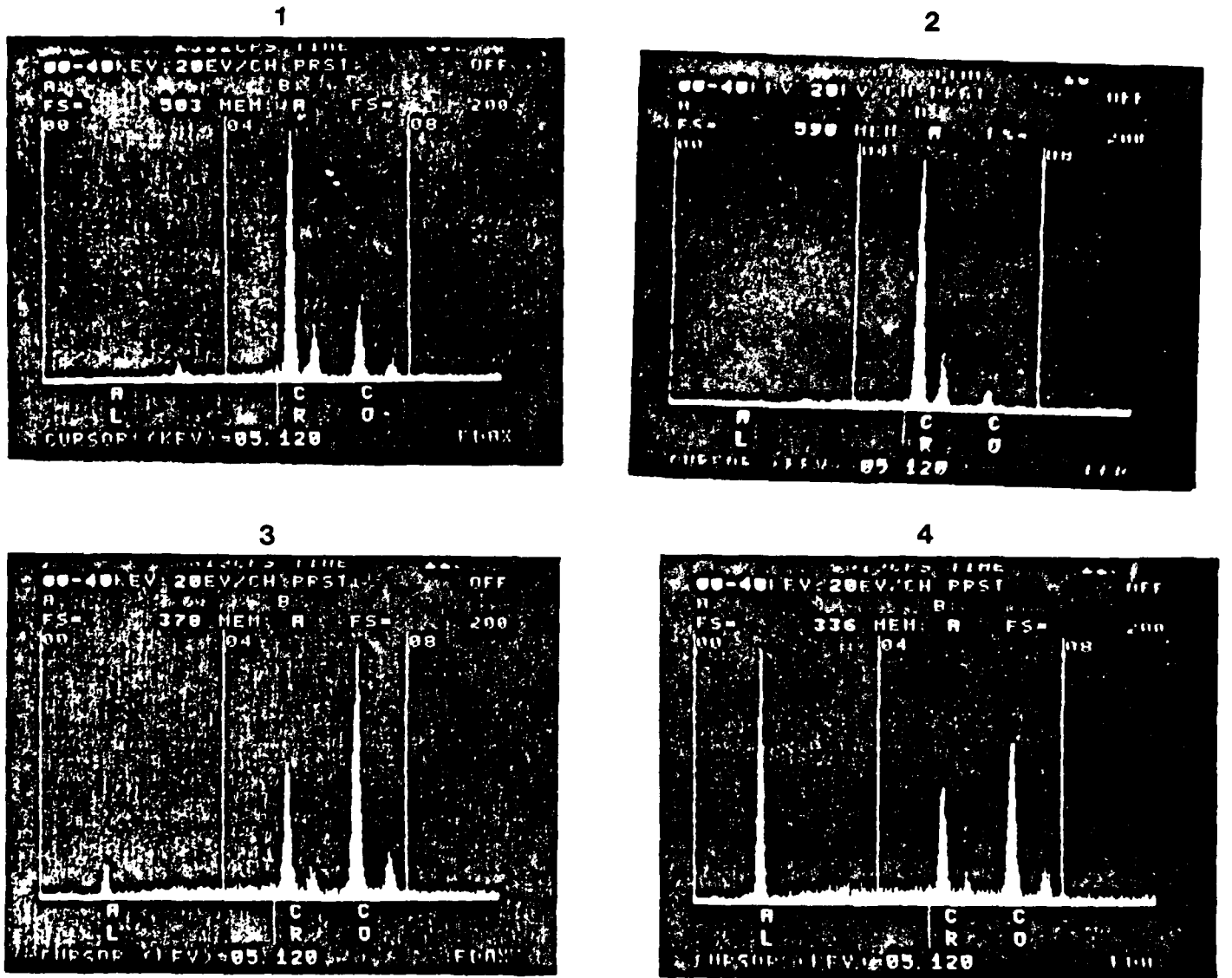

Figure 27. EDAX spectra from indicated locations in Figure 26.

Figure 28. Cross-sections of Mg-implanted CoCrAl oxidized for 48 hours at 950°C in oxygen.

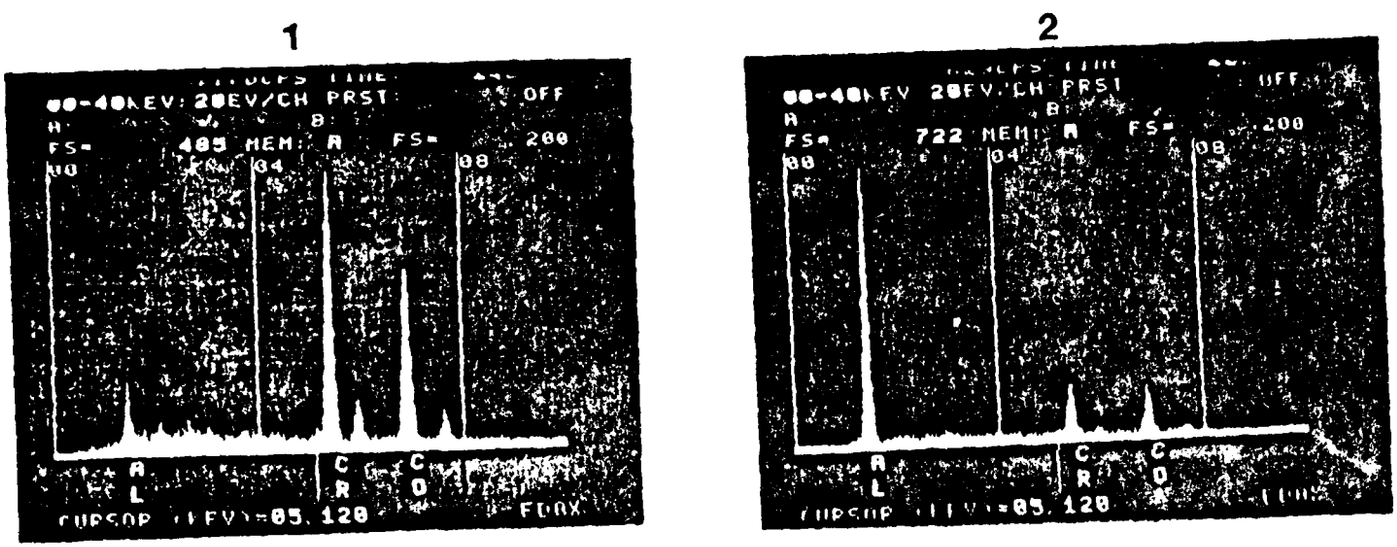

Figure 29. EDAX spectra from indicated locations in Figure 28b.

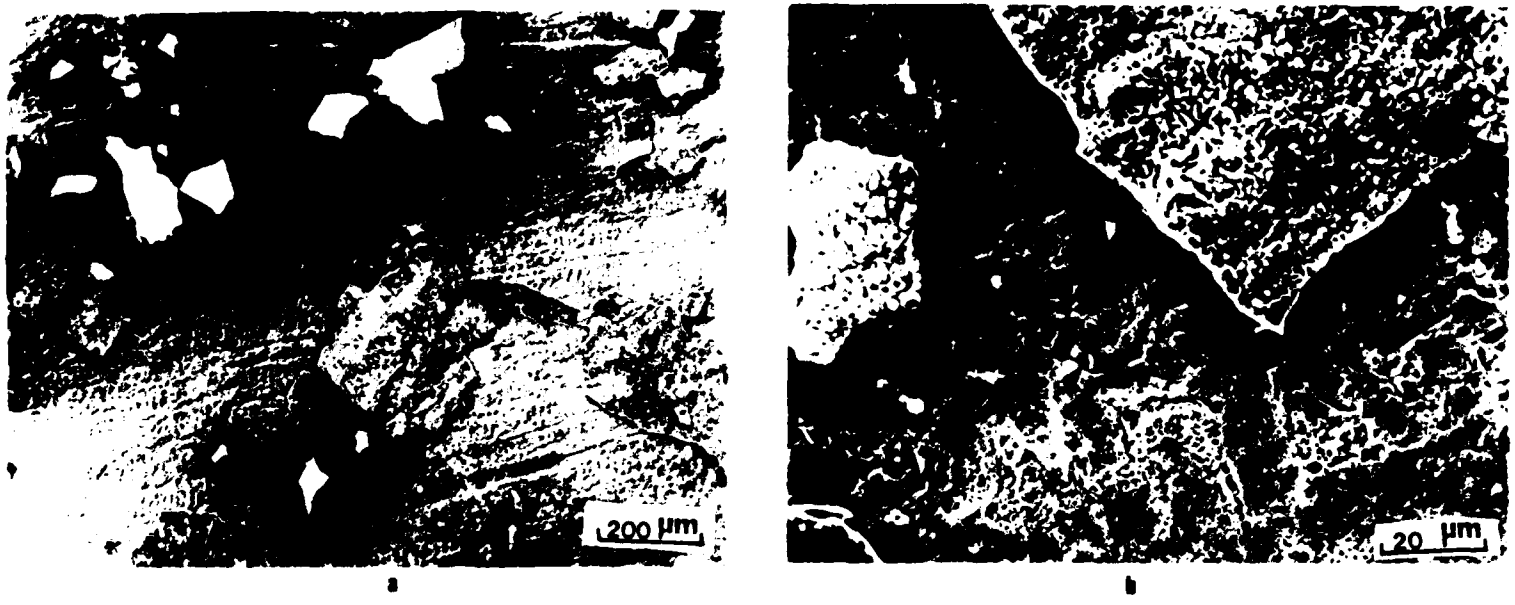

Figure 30. Surface of Mg-implanted CoCrAl oxidized for 48 hours at 950°C.

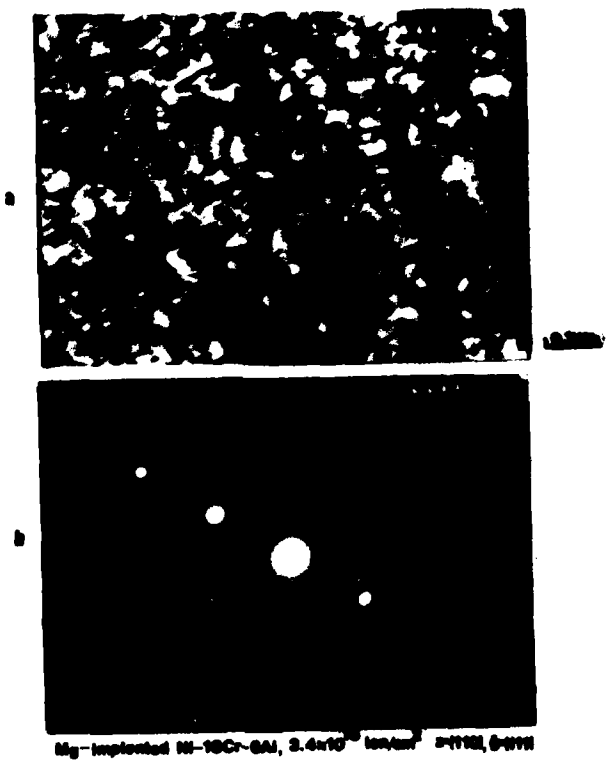

Figure 31. Transmission electron micrograph of implanted region of Mg-implanted NiCrAl (a) and corresponding selected area diffraction pattern.

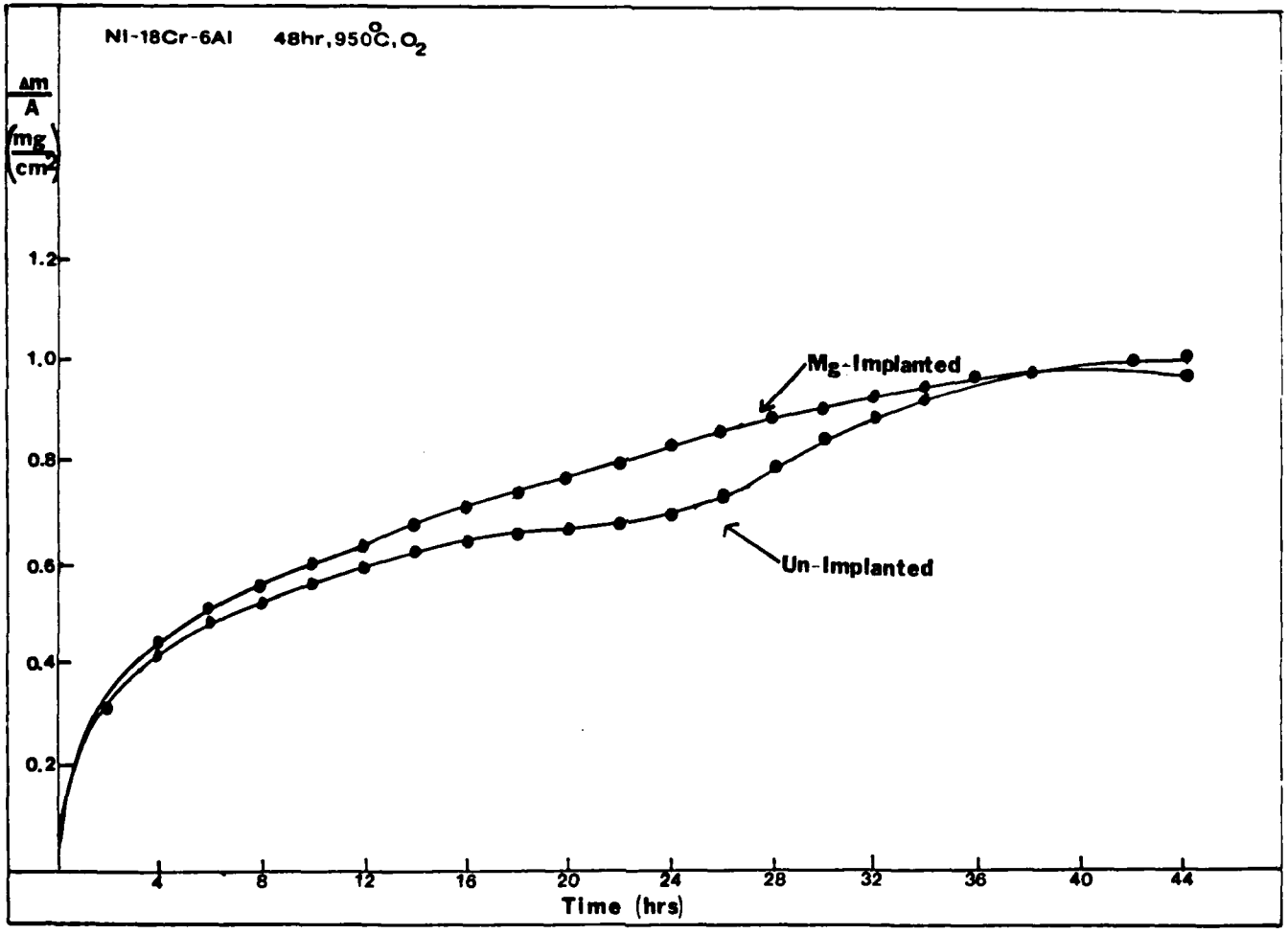

Figure 32. Oxidation rates of Ni-18 Cr-6 Al and Mg-implanted Ni-18 Cr-6 Al

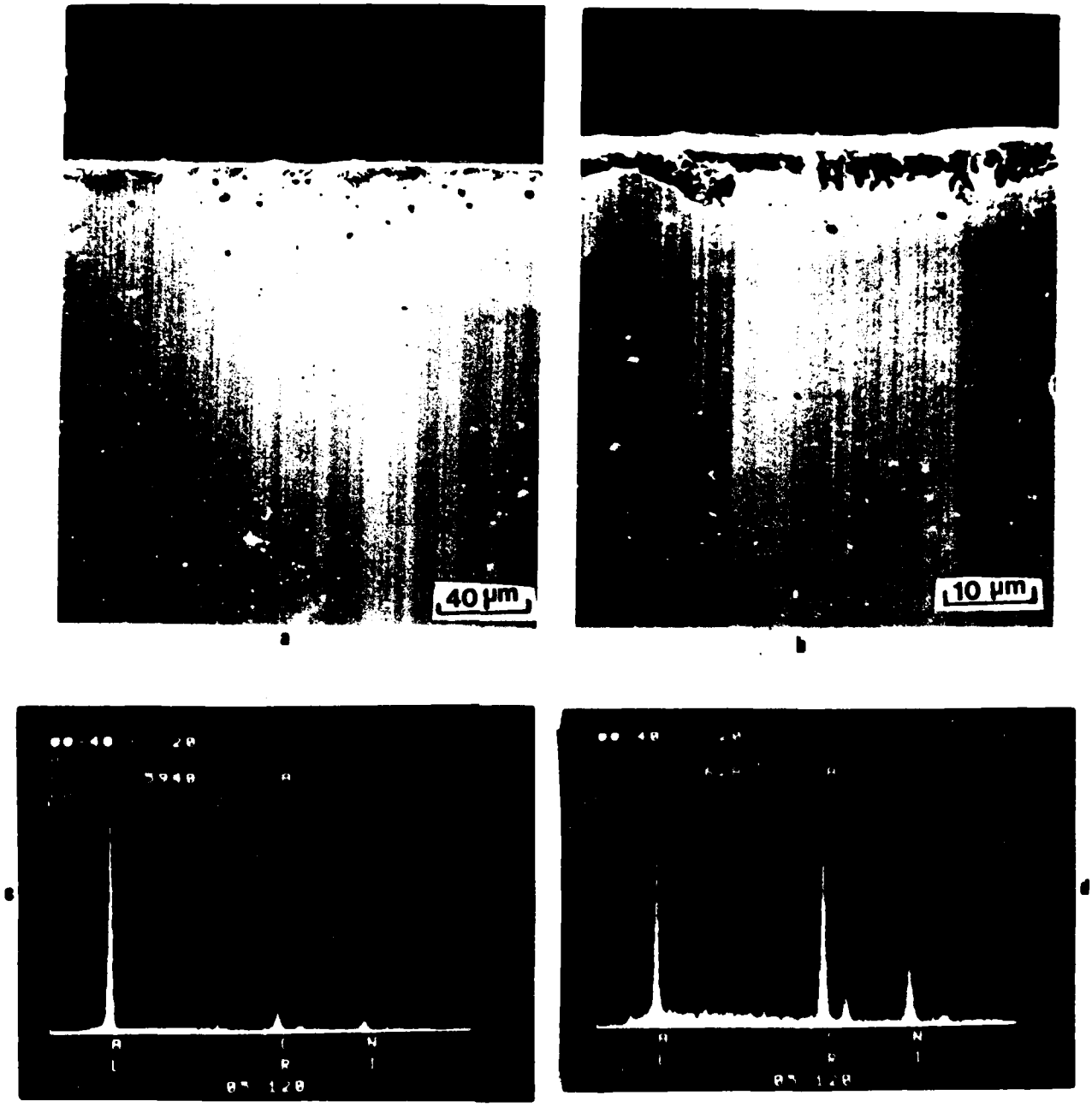

Figure 33. Cross sections of NiCrAl oxidized for 48 hours at 950°C in air (a,b) and EDAX spectra of the inner oxide scale (c) and the outermost oxide (d).

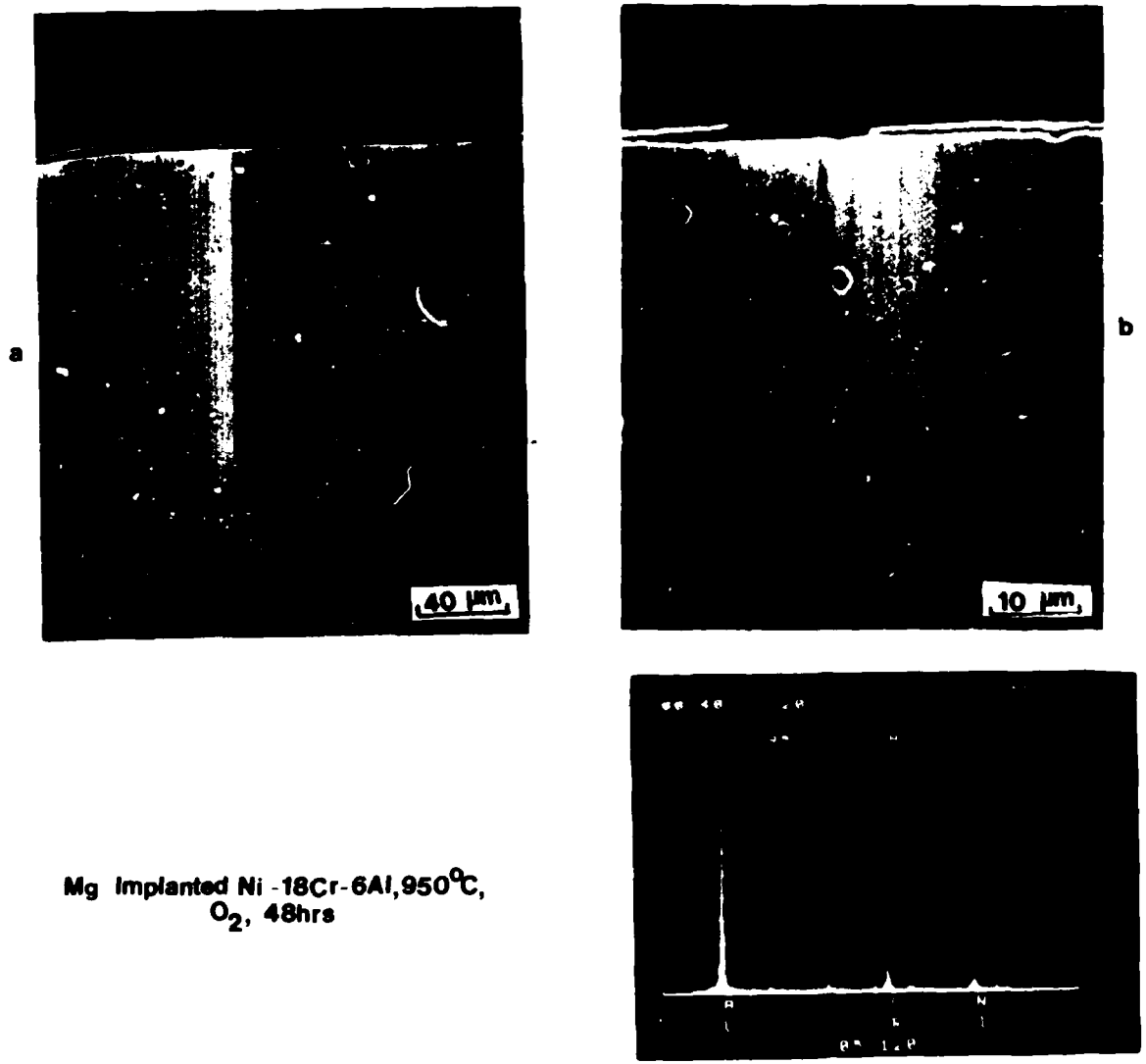

Figure 34. Cross-sections of Mg-implanted NiCrAl oxidized for 48 hours at 950°C in oxygen (a,b) and EDAX spectrum of the scale (c).

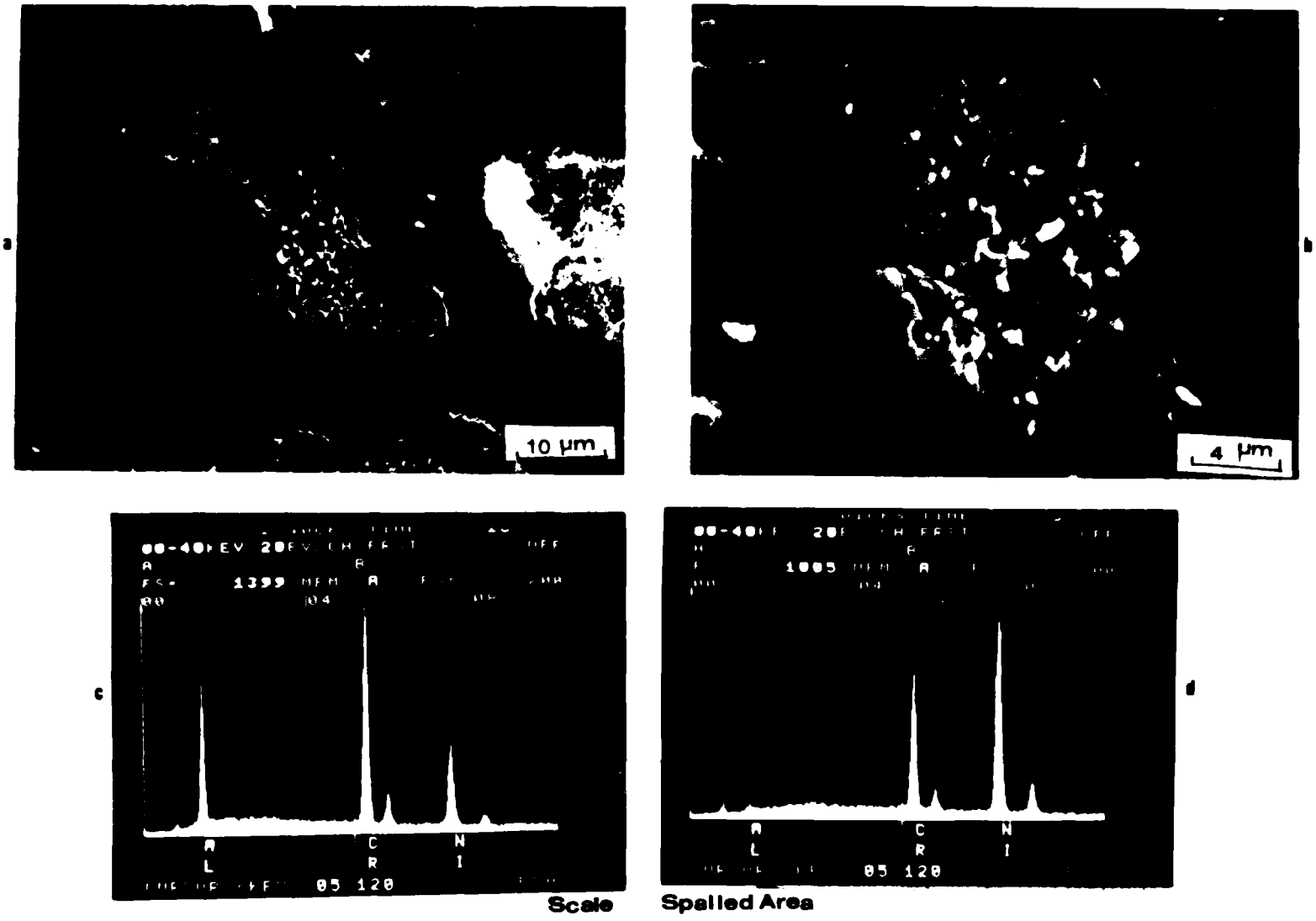

Figure 35. Surface of NiCrAl oxidized for 48 hours at 950°C in oxygen (a,b) and EDAX spectra of the scale (c) and spalled area (d).

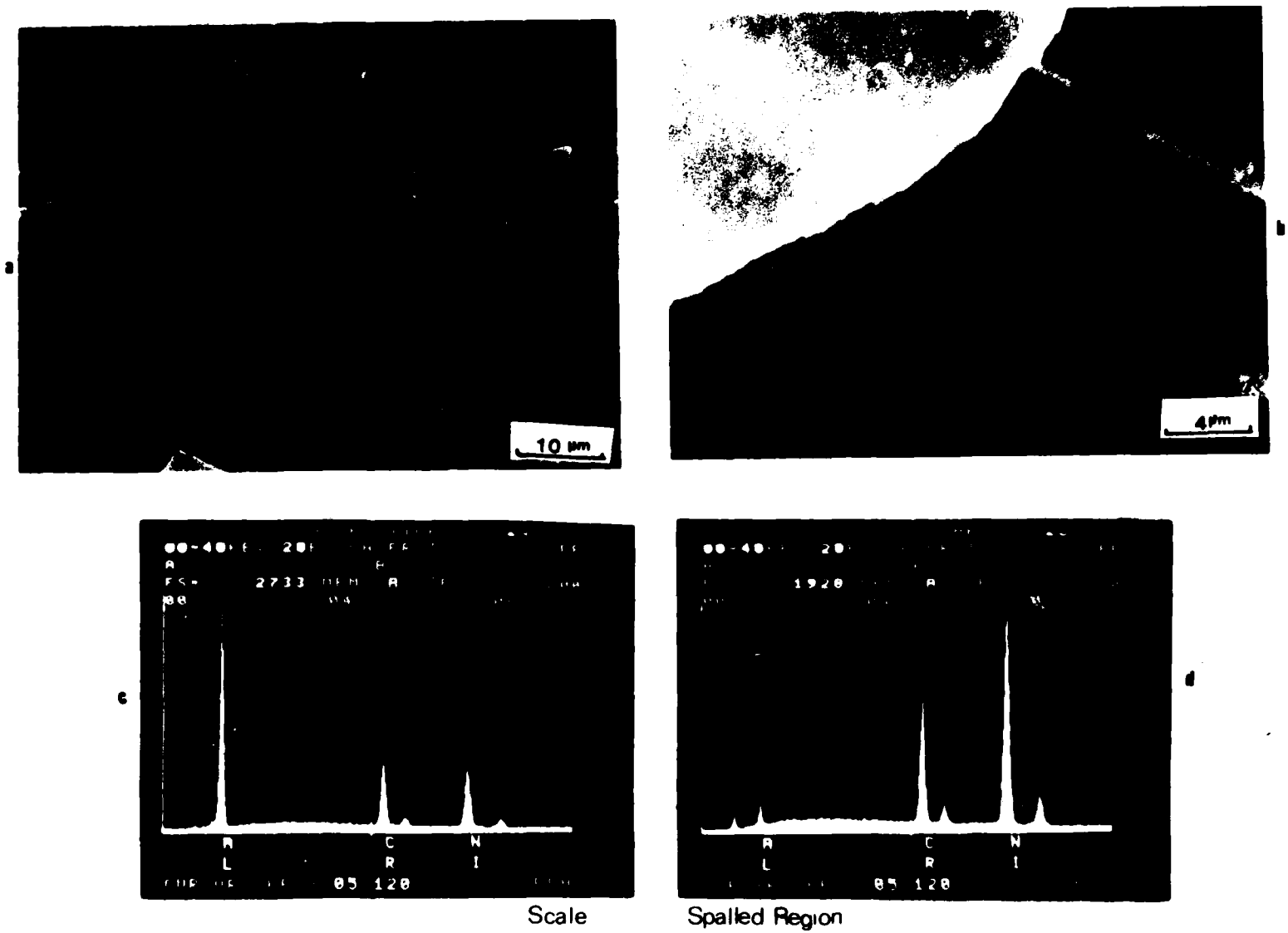

Figure 36. Surface of Mg-implanted NiCrAl oxidized for 48 hours at 950°C in oxygen (a,b) and EDAX spectra of the scale (c) and spalled area (d).

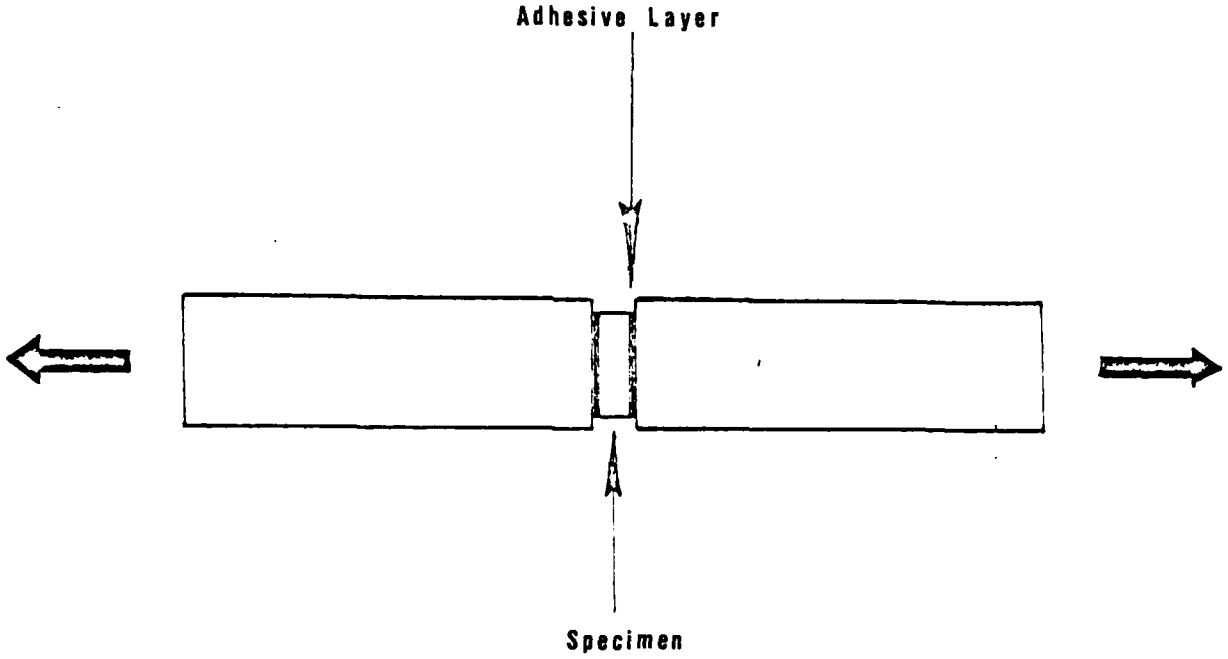

Figure 37. Schematic diagram of the test assembly for measuring the load required to separate an oxide from its substrate.

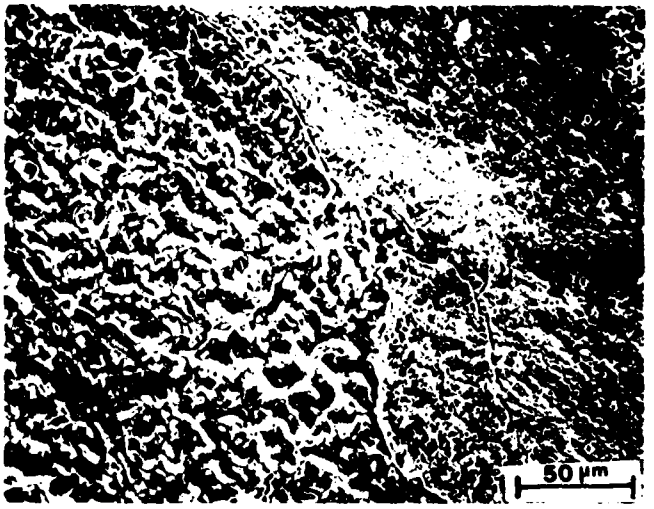

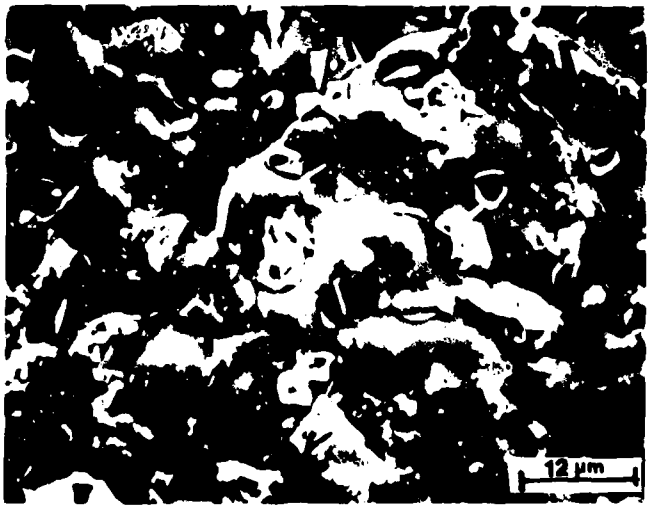

Figure 38. Surface of Ni specimen oxidized for 82 hours at 1100°C from which the scale has been pulled.

Figure 39. Surface of NiCoCrAlY oxidized at 1150°C from which the scale has been pulled.

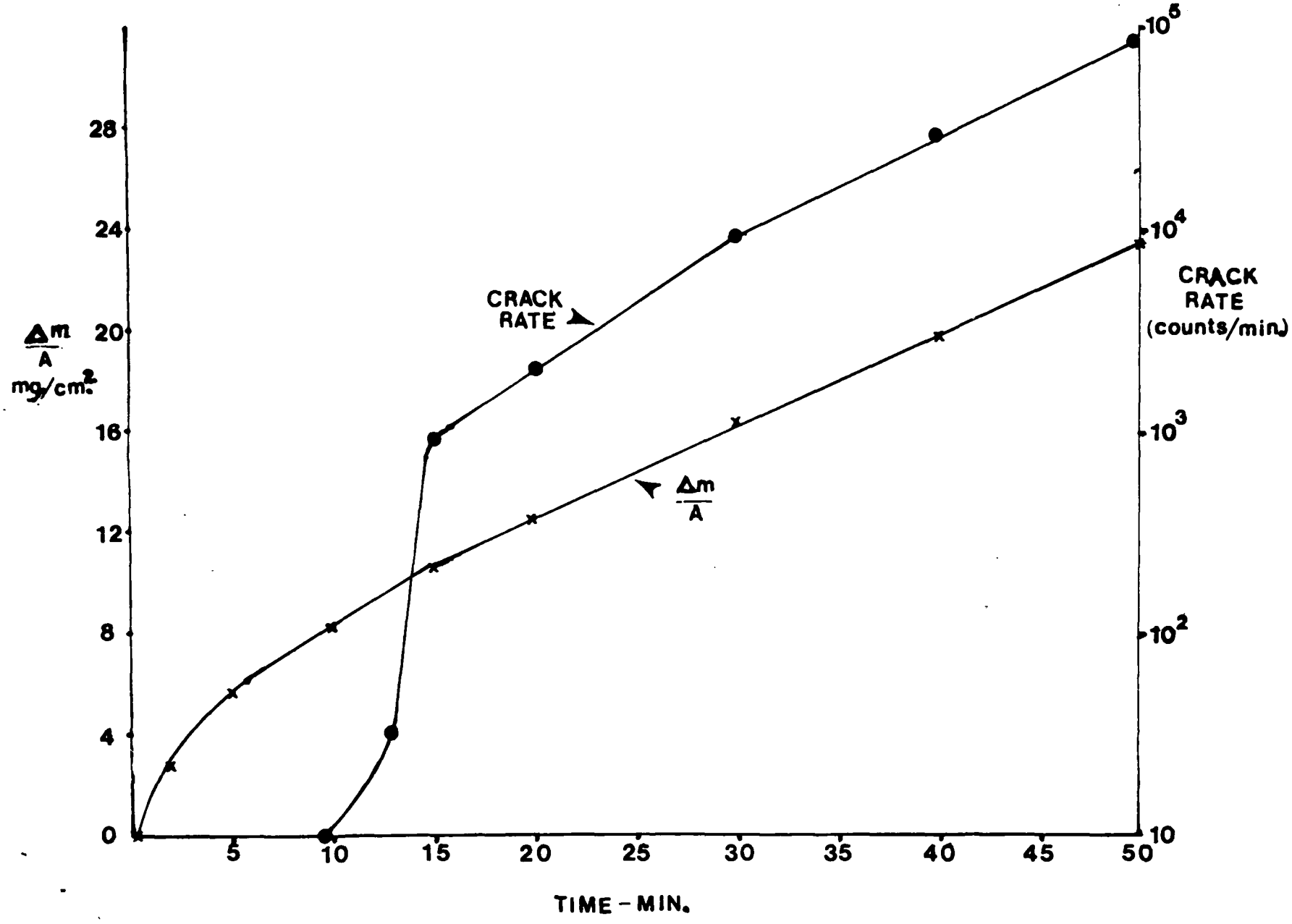

Figure 40. Oxidation rate of Nb at 800°C in air and the corresponding scale cracking rate as measured by acoustic emission.


DATE
ILME
8